Effects of Induced Streambed Infiltration on Water Levels In Wells During Aquifer Tests

by WILLIAM C. WALTON and EARL A. ACKROYD

The work upon which this publication is based was supported by funds provided by the United States Department of the Interior as authorized under the Water Resources Research Act of 1964, Public Law 88-379

JUNE 1966
MINNEAPOLIS, MINNESOTA

WATER RESOURCES RESEARCH CENTER
UNIVERSITY OF MINNESOTA
GRADUATE SCHOOL

CONTENTS

ILLUSTRATIONS

TABLES

FOREWORD

This Bulletin is published in furtherance of the purposes of the Water Resources Research Act of 1964, signed into law on July 17, 1964. The purpose of the Act is to stimulate, sponsor, provide for, and supplement present programs for the conduct of research, investigations, experiments, and the training of scientists in the field of water and resources which affect water. The Act is promoting a more adequate national program of water resources research by furnishing financial assistance to non-federal research.

The Act provides for establishment of Water Resources Research Institutes or Centers at Universities throughout the Nation. On September 1, 1964, a Water Resources Research Center was established in the Graduate School as an interdisciplinary component of the University of Minnesota. The Center has the responsibility for unifying and stimulating University water resources research through the administration of funds covered in the Act and made available by other sources; coordinating University research with water resources programs of local, State and Federal agencies and private organizations throughout the State; and assisting in training additional scientists for work in the field of water resources through research.

This report is the second in a series of publications designed to present information bearing on water resources research and the results of some of the research sponsored by the Center. Principal Investigators of other research projects conducted by components of the University may choose to report the results of their research in this series of publications.

In the present investigation, electric analog computers are employed to study the effects of recharge by the seepage of water through streambeds on water levels in aquifers. The need for continuing research on induced streambed infiltration is clearly apparent, and the Center is planning to carry forward additional studies in this field.

Effects of Induced Streambed Infiltration on Water Levels in Wells During Aquifer Tests

by W. C. Walton[a] and E. A. Ackroyd[b]

ABSTRACT

The aquifer test, involving a production well and several observation wells near a stream, is one of the most useful tools available to hydrologists for the determination of the effects of induced streambed infiltration on water levels in aquifers. In presently available analytical treatments of flow problems associated with induced infiltration, recharge by the influent seepage of surface water is commonly simulated by use of a hypothetical image well. The assumption is made that water levels in the aquifer will behave the same whether recharge occurs over an area or through an image well.

Electric analog computers, in which the streambed is simulated as an area of recharge in accordance with natural conditions instead of as a recharging image well, were used to appraise the accuracy of estimated effects of induced infiltration on water levels based on the image well theory. Electric analog computers for two aquifer test sites for which field data are available were constructed. The selected aquifer tests involve the two extreme aquifer-stream situations, i.e., the case where the cone of depression spreads beneath and beyond the entire streambed and the case where the cone of depression spreads only part way beneath the streambed. The analog computers consist of analog models and excitation-response apparatus. The analog models are regular arrays of resistors and capacitors and are scaled-down versions of aquifer-stream situations. The excitation-response apparatus consists of a power supply, waveform generator, pulse generator and an oscilloscope.

It is concluded that, during induced infiltration aquifer tests, the image-well theory closely describes drawdowns on the land sides of streams with a high degree of accuracy whether the cone of depression spreads beneath and beyond or only part way beneath the streambed. Drawdowns beneath or beyond the streambed and the streambed areas of infiltration based on the image-well theory are not those which are observed in the field. However, the streambed infiltration rates per foot of head loss based on hypothetical drawdowns beneath streambeds and streambed areas of infiltration computed with the image-well theory seem to be empirically correct.

Attention is directed to the need for the installation of observation wells within and beyond the streambed for use during aquifer tests. Additional research pertaining to recharge through streambeds partially penetrating aquifers and having finite widths, under varying stream-stage and water-level conditions is needed.

---

[a] Director, Water Resources Research Center and Professor of Geology and Geophysics
[b] Research Fellow, Water Resources Research Center

INTRODUCTION

In recent years, ground-water supplies using induced infiltration of surface water as a source of recharge have been extensively developed especially in areas in north-central United States that were covered by or adjacent to the Pleistocene ice sheets. In the glaciated areas or closely adjacent to them valleys cut into the bedrock often contain limited to extensive sand and gravel outwash aquifers. At many places the bedrock valleys and the outwash patterns coincide with present stream valleys and the sand and gravel aquifers under heavy pumping conditions are subject to recharge from streamflow.

Before the ground-water resources of undeveloped aquifers recharged by induced streambed infiltration can be appraised, the induced infiltration rates of streambeds in addition to the hydrogeologic properties and boundaries of aquifers must be evaluated. The aquifer test, involving a production well and several surrounding observation wells near a stream, is one of the most useful tools available to hydrologists for the determination of the infiltration rates of streambeds and the hydrogeologic properties of aquifers.

Methods for determining the hydrogeologic properties of an aquifer and for evaluating the effects of induced infiltration on the water levels in wells have been described by Kazmann (1948), Glover and Balmer (1954), Rorabaugh (1956), Hantush (1959, 1964, and 1965), and Schaefer and Kaser (1965). Approximate methods of analysis of aquifer test data to enable the ground-water hydrologist to obtain estimates of the average induced infiltration rate of a streambed and to estimate the amount of potential recharge from induced infiltration of surface water were described by Walton (1963). The percentage of pumped water being diverted from a stream, the area of the streambed through which influent seepage of surface water occurs, and the average head loss due to the vertical percolation of water through the streambed may be estimated with the image-well theory. The location of the image well which simulates induced infiltration is determined by analysis of the stabilized cone of depression of the production well which may expand beneath and beyond the entire streambed.

In the present investigation, the accuracy and reliability of induced infiltration rates and the effects of induced infiltration on the water levels in wells estimated by use of the image-well theory are appraised with electric analog computers. In the electric analog computers, the streambed is simulated as an area of recharge in accordance with natural conditions instead of as a recharging image well. Induced infiltration rates and water-level declines for two aquifer-stream situations determined with electric analog computers and the image-well theory are compared. In addition, the effects of a stream-stage change on water levels in a selected aquifer are determined with electric analog computers.

THEORY OF INDUCED INFILTRATION

The cone of depression created by pumping a well near a stream which is hydraulically connected to an aquifer is distorted. The hydraulic gradients between the stream and the pumped well are steep in comparison to those on the land side of the well. The flow toward the well is greatest on the river side of the well, and under equilibrium conditions most of the water discharged from the well is derived from streamflow.

When the well is pumped, water is first withdrawn from storage within the aquifer in the immediate vicinity of the well. The cone continues to spread, drawing water from storage within an increasing area of influence. Water levels in the vicinity of the stream are lowered, and more and more of the water which under natural conditions would have discharged into the stream as ground-water runoff, or into the atmosphere as evapotranspiration, is diverted toward the well. Ultimately, water levels may be lowered below all or part of the surface of the stream in the immediate vicinity of the well, and the aquifer is recharged by the influent seepage of surface water.

If recharge by the induced infiltration of surface water from the reach of the stream in the immediate vicinity of the well cannot keep pace with the discharge, the cone of depression spreads up and down stream. The cone of depression continues to grow until it intercepts a sufficient area of the streambed and creates sufficient head differentials so that induced infiltration balances discharge. If the permeability of the streambed is high and the stream is wide, the cone of depression may extend only part way beneath the streambed; if the permeability of the streambed is low and the stream is narrow, the cone of depression may continue to expand beneath and beyond the entire streambed.

Darcy in 1856 proved that the quantity of water percolating through the interstices of a column of sand is directly proportional to the permeability of the sand and to the difference in head at the ends of the column. The infiltration rate of a streambed is, therefore, a direct function of permeability and head. Recharge from streamflow is directly proportional to the permeability of the streambed and to the difference between water levels in the aquifer immediately below the streambed and the surface of the stream, until the water table has declined below the streambed.

Recharge by the influent seepage of surface water takes place over an area of the streambed. However, to make flow problems associated with induced infiltration amenable to mathematical treatment, the area is replaced by a line source. The assumption is made that water levels in the aquifer will behave the same whether recharge occurs over an area or along a line. According to the image-well theory, the effect of a line source on the drawdown in an aquifer, as a result of pumping from a well near the line source, is the same as though the aquifer were infinite and a like recharging well were located across the line source, on a line at right angles thereto and at the same distance from the line source as the real well.

Consider an aquifer bounded on one side by a recharge boundary as shown in figure 1A. The cone of depression cannot spread beyond the stream. The condition is established that there shall be no drawdown along an effective line of recharge somewhere offshore. The imaginary hydraulic system of a well and its image counterpart in an infinite aquifer shown in figure 1B satisfies the foregoing boundary condition. A recharging image well has been placed directly opposite and at the same distance from the stream as the real well. The recharging image well operates simultaneously and at the same rate as the real well. The resultant real cone of depression is the arithmetic summation of the components of the real cone of depression

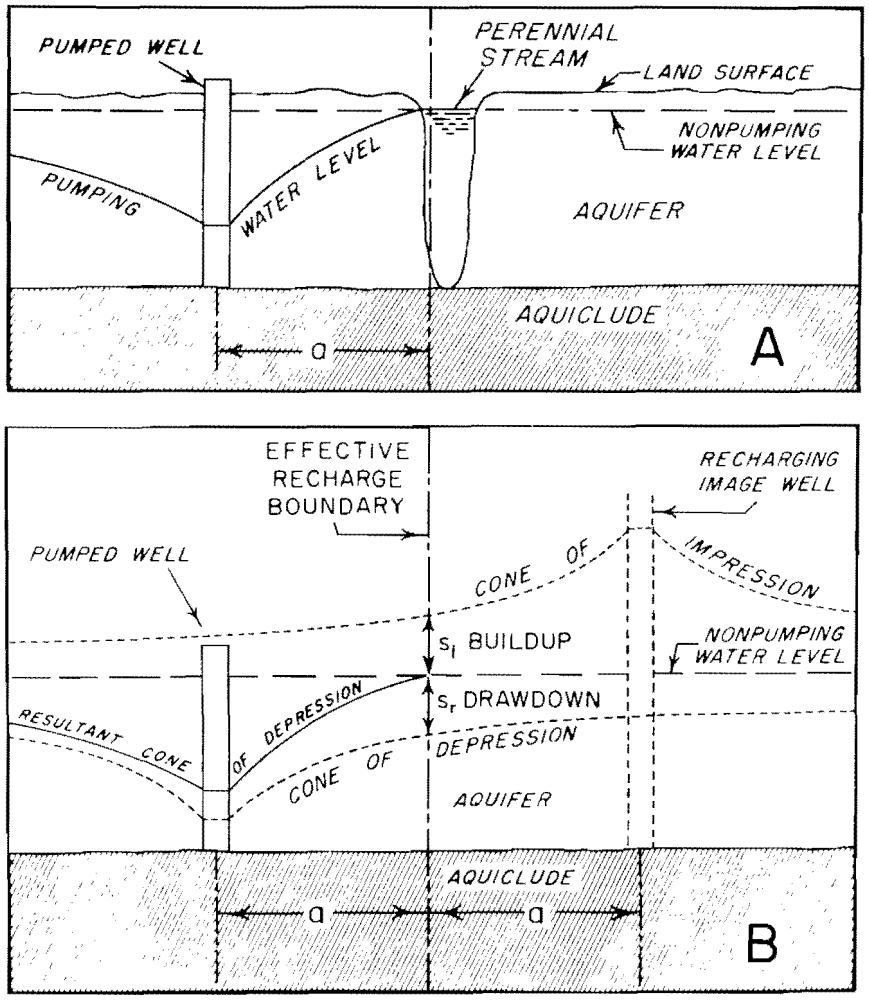

(AFTER FERRIS, ET AL, 1962)

Figure 1. Diagrammatic representation of the image-well theory as applied to a recharge boundary.

and the image well cone of impression as shown in figure 1B. The resultant profile of the real cone of depression is steeper on the river side of the real well and flatter on the land side of the real well than it would be if no boundary was present. A generalized plan view of the flow net in the vicinity of a discharging well near a recharge boundary is shown in figure 2.

It can be shown by the development of the nonequilibrium formula (Theis, 1935) that the drawdown in an aquifer at any point for the conditions set forth above is:

$$s = \frac{528\ Q \log_{10} \frac{r_i}{r_p}}{T} \tag{1}$$

where: s = drawdown at observation well, in feet (ft); Q = discharge of pumped well, in gallons per minute (gpm); r_i = distance from image well to observation well, in ft; r_p = distance from pumped well to observation well, in ft; T = coefficient of transmissibility in gallons per day per foot (gpd/ft).

This equation was expressed in terms of the distance between the pumped well and the line source or recharge boundary by Rorabaugh (1956) as:

$$s = \frac{528\ Q \log_{10} \frac{\sqrt{4a^2 + r_p^2 - 4ar_p \cos\phi}}{r_p}}{T} \tag{2}$$

where: a = distance from pumped well to recharge boundary, in ft; ϕ = angle between a line connecting pumped and image wells and a line connecting pumped well and observation well.

For the particular case where the observation well is on a line parallel to the recharge boundary the following equation (Rorabaugh, 1956) applies:

$$s = \frac{528\ Q \log_{10} \left(\frac{\sqrt{4a^2 + r_p^2}}{r_p} \right)}{T} \tag{3}$$

For the particular case where the observation well is on a line perpendicular to the recharge boundary and on the river side, the following equation (Rorabaugh, 1956) applies:

$$s = \frac{528\ Q \log_{10} \left| \frac{(2a - r_p)}{r_p} \right|}{T} \tag{4}$$

Distance to Recharge Boundary and Hydrogeologic Properties of Aquifer

The stabilized cone of depression of a production well near a recharge boundary can be described and the area of influence of pumping can be delineated with equation 2 provided the distance "a" and the coefficient of transmissibility are known. These basic factors often can be determined from aquifer test data.

Suppose that a pumped well, near a recharge boundary and in an otherwise infinite aquifer, homogeneous and isotropic in nature, is pumped continuously until water levels stabilize, and that drawdowns are measured in several observation wells on a line through the pumped well and parallel to the recharge boundary. In many

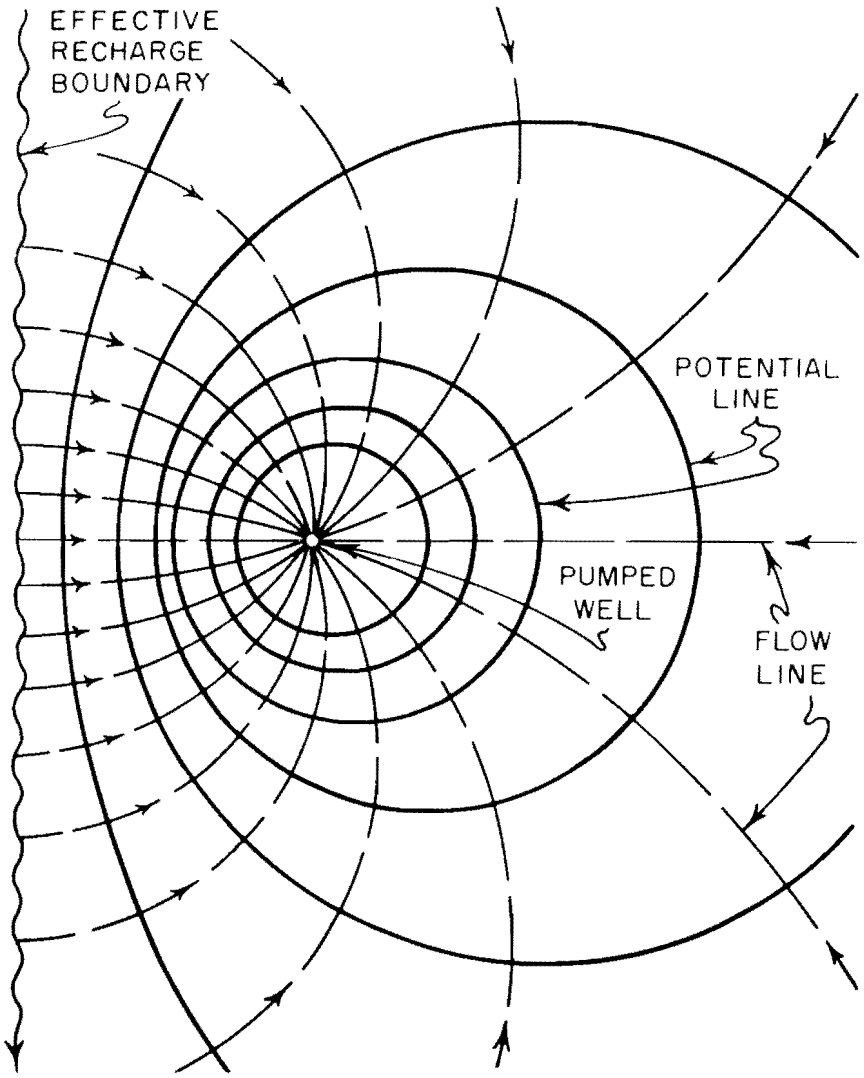

Figure 2. Generalized flow net showing flow lines and potentiol lines in the vicinity of a discharging well near a recharge boundary.

cases the line of recharge cannot be located with observation well time-drawdown graphs and the image-well theory because most time-drawdown data are affected by recharge from the stream and slow gravity drainage of interstices. However, the data on the total drawdowns in the observation wells can be used to determine the distance "a".

The coefficient of transmissibility also often can be determined from distance-drawdown data for observation wells on a line parallel to the recharge boundary. Provided that the observation wells are not too close to the recharge boundary and not too far from the pumped well, the hydraulic gradient of the profile of the stabilized cone of depression through the wells will not be distorted to any appreciable degree. The wells are approximately equidistant from the image well associated with the recharge boundary, and the effects of induced infiltration on drawdowns are approximately equal at all wells. Thus, the distance-drawdown data for wells on a line parallel to the stream closely describe the hydraulic gradient towards the pumped well that would exist if the aquifer were infinite in areal extent. A semi-logarithmic plot of total drawdowns in the observation wells will yield a straight-line graph. The slope of the straight line is substituted into the following equation to compute the coefficient of transmissibility (see Walton, 1962):

$$T = \frac{528\ Q}{\Delta s} \tag{5}$$

where: T = coefficient of transmissibility, in gpd/ft; Q = discharge of pumped well, in gpm; Δs = drawdown difference per log cycle as determined from distance-drawdown graph, in ft.

Although the hydraulic gradient is not distorted, the total drawdowns in the observation wells are much less than they would be under infinite aquifer conditions because of the effects of recharge, and the coefficient of storage of the aquifer cannot be determined from the distance-drawdown graph.

If T is known, the distance "a" can be computed on the basis of the total drawdown in each observation well on a line parallel to the stream and the following equation (Rorabaugh, 1956):

$$\frac{\log_{10} \sqrt{4a^2 + r_p^2}}{r_p} = \frac{Ts}{528\ Q} \tag{6}$$

where: a = distance from pumped well to recharge boundary, in ft; r_p = distance from pumped well to observation well, in ft; Q = discharge of pumped well, in gpm; T = coefficient of transmissibility, in gpd/ft. The ratio of the drawdowns in any two observation wells on a line parallel to the stream (see Rorabaugh, 1956) also may be used to determine "a".

Equations 1 through 6 assume that the cone of depression has stabilized, water is no longer taken from storage within the aquifer, and equilibrium conditions prevail. The pumping period required to reach approximate equilibrium conditions can be computed by using the following equation (see Foley, Walton and Drescher, 1953):

$$t_e = \frac{3.26a^2S}{T\ \epsilon\ \log_{10}\left(\frac{2a}{r_p}\right)^2} \tag{7}$$

where: t_e = time after pumping starts before equilibrium conditions prevail, in days; S = coefficient of storage, fraction; ϵ = deviation from absolute equilibrium (arbitrarily assumed to be 0.05).

The effects of slow gravity drainage of interstices under water-table conditions and leakage through an aquitard under leaky-artesian conditions closely resemble the effects of recharge by induced infiltration. The mere fact that the cone of depression stabilizes is not positive proof that induced infiltration is occurring. The decrease in the time-rate of drawdown can be attributed either to the effects of slow gravity drainage, effects of leakage through an aquitard, or effects of induced infiltration if the effects of partial penetration are excluded. Rorabaugh (1956) gives methods for proving whether or not water levels stabilize because of the effects of slow gravity drainage.

The nonequilibrium formula and computed values of T and "a" can be used to determine the coefficient of storage. Drawdown in an aquifer affected by recharge from a line source is from the nonequilibrium formula and the image-well theory given by the following equation:

$$s = \frac{114.6\ Q}{T}\ [W(u_p) \quad \cdot W(u_i)] \tag{8}$$

where:

$$W(u_{p,i}) = \int_u^\infty \frac{e^{-u}}{u}\ du = -.05772 \quad \log_e u + u \quad \frac{u^2}{2.2!} + \frac{u^3}{3.3!} \quad \frac{u^4}{4.4!} \ldots \text{etc.} \tag{9}$$

$$u_p = \frac{1.87\ r_p^2 S}{Tt} \tag{10}$$

$$u_i = \frac{1.87\ r_i^2 S}{Tt} \tag{11}$$

and s = drawdown in observation well, in ft; Q = discharge of pumped well, in gpm; T = coefficient of transmissibility, gpd/ft; r_i = distance from observation well to image well associated with recharge boundary, in ft; r_p = distance from observation well to pumped well, in ft; t = time after pumping started, in days; and S = coefficient of storage, fraction.

Several assumed values of the coefficient of storage are substituted into equations 10 and 11 for computation of u_p and u_i. Corresponding values of $W(u_p)$ and $W(u_i)$ are obtained from a table of $W(u)$ versus u (see Walton, 1962) and are substituted into equation 8 to determine drawdowns. The computed drawdowns are then compared with actual drawdowns in observation wells, and that coefficient of storage which was used to compute drawdowns equal to actual drawdowns is assigned to the aquifer.

In some cases, time-drawdown data are not affected by the stream until an appreciable time after pumping started. Under these conditions, the distance "a" can be computed with the law of times defined by Ingersoll, Zobel, and Ingersoll (1948).

If the time intercept of a given drawdown in an observation well caused by pumping a well at a given distance is known, and if the time intercept of an equal amount of divergence of the time-drawdown curve caused by the effect of the image well is also known, it is possible to determine the distance from the observation well to the image well using the following formula which expresses the law of times:

$$r_i = r_p \sqrt{t_i/t_p} \tag{12}$$

where: r_i = distance from image well to observation well, in ft; r_p = distance from

pumped well to observation well, in ft; t_p = time after pumping started, before the boundary becomes effective, for a particular drawdown to be observed, in days; and t_i = time after pumping started, after the boundary becomes effective, when the divergence of the time-drawdown curve from the type curve, under the influence of the image well, is equal to the particular value of drawdown at t_p, in days.

Gravity drainage of interstices decreases the saturated thickness and therefore the coefficient of transmissibility of the aquifer. Under water-table conditions, observed values of drawdown must be compensated for the decrease in saturated thickness before the data can be used to determine the hydrogeologic properties of the aquifer and the distance "a". The following equation derived by Jacob (1944) is used to adjust drawdown data for decreases in the coefficient of transmissibility:

$$s' = s - \left(\frac{s^2}{2m}\right) \tag{13}$$

where: s' = drawdown that would occur in an equivalent artesian aquifer, in ft; s = observed drawdown under water-table conditions, in ft; and m = initial saturated thickness of aquifer, in ft.

Amount of Induced Infiltration and Streambed Area of Infiltration

If the hydrogeologic properties of the aquifer, T and S, and the distance "a" are known, the percentage of pumped water being diverted from a stream can be computed with the following equation derived by Theis (1941):

$$P_r = \frac{2}{\pi} \int_0^{\pi/2} e^{-f} \sec^2 u\ du \tag{14}$$

where:

$$u = \tan^{-1}\frac{x}{a} \qquad f = \frac{1.87a^2S}{Tt} \tag{15}$$

and P_r = percentage of pumped water being diverted from the stream; T = coefficient of transmissibility, in gpd/ft; S = coefficient of storage, fraction; a = distance from pumped well to recharge boundary, in ft; t = time after pumping started, in days; and x = distance along recharge boundary measured from perpendicular joining real and image wells, in ft.

Figure 3A gives values of P_r for various values of f and shows therefore the percentage of pumped water being diverted from the stream. The amount of recharge by induced infiltration is then given by the following equation:

$$Q_r = \frac{Q\ P_r}{100} \tag{16}$$

where: Q_r = amount of induced infiltration, in gpm; and Q = discharge of pumped well, in gpm.

The area of the streambed through which influent seepage of surface water is occurring can be determined from data on water-level declines in observation wells terminating immediately below the streambed or with equation 8. The locations of the pumped well, the image well associated with the recharge boundary, and the streambed are drawn to scale on a map. Several points within the stream-

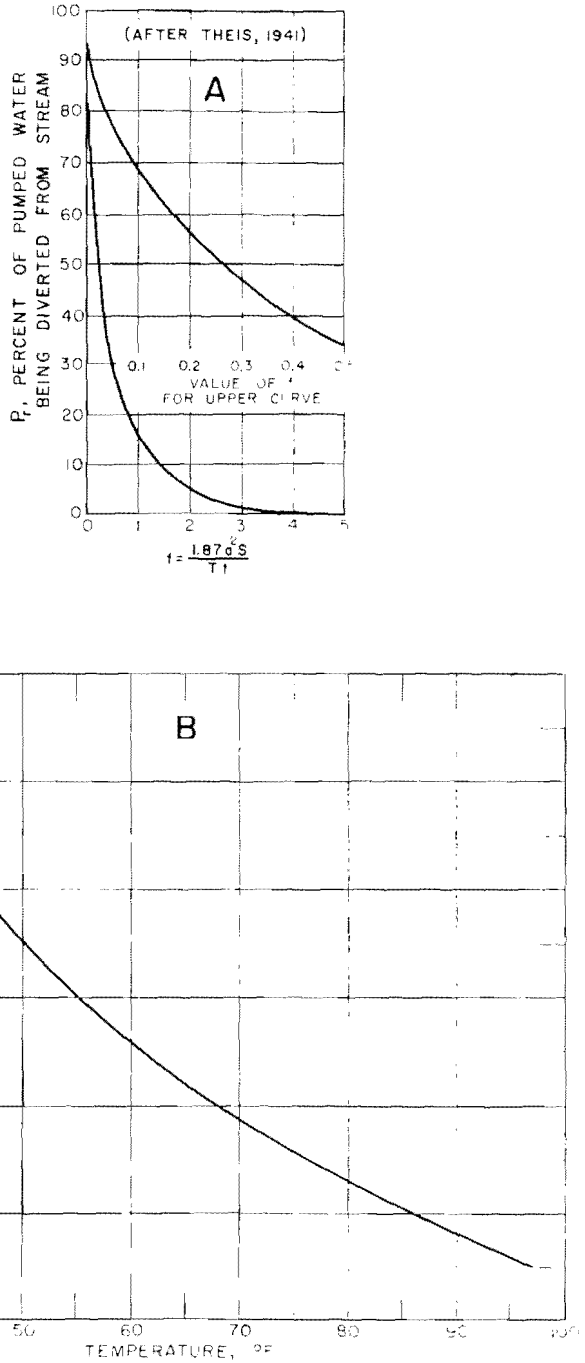

Figure 3. Relationship between P_r and f (A) and coefficient of viscosity and temperature (B).

bed that are equidistant up and down stream from the pumped well are selected for computations of drawdown. The distances between the selected points, the pumped well, and the image well are scaled from the map. Values of drawdown at the selected points are then computed with equation 8. The reach of the streambed, L_r, within the area of influence of pumping is ascertained by noting the location of the points up and down stream where drawdown is negligible (say ≤ 0.01 ft). The area of induced infiltration, A_r, is then the product of L_r and the average distance between the shore line and the recharge boundary or the average width of the streambed, depending upon the position of the recharge boundary.

Induced Infiltration Rate

When Q_r and A_r are known, the induced infiltration rate of the streambed per unit area can be computed with the following equation:

$$I_a = \frac{6.3 \times 10^5 \, Q_r}{A_r} \qquad (17)$$

where: I_a = average infiltration rate of streambed per unit area, in gallons per day per acre (gpd/acre); Q_r = amount of induced infiltration, in gpm; and A_r = streambed area of infiltration, in square feet (sq ft).

The average head loss, s_r, due to the vertical percolation of water through the streambed can be determined from data for observation of wells installed within the streambed area of infiltration at depths just below the streambed. In many cases the installation of observation wells in the stream channel is impractical, and s_r must be estimated with equation 8 and the hydrogeologic properties and position of the recharge boundary determined by aquifer test analysis. The drawdowns at many points within the streambed area of infiltration are computed with equation 8; the average of the computed drawdowns is the approximate average s_r within the streambed area of infiltration. The average infiltration rate of the streambed per unit area per foot of head loss can be estimated by use of the following equation:

$$I_h = \frac{I_a}{s_r} \qquad (18)$$

where: I_h = average infiltration rate of streambed per unit area per foot of head loss, in gallons per day per acre of streambed per foot of head loss (gpd/acre/ft); I_a = average infiltration rate of streambed per unit area, in gpd/acre; s_r = average head loss within streambed area of infiltration, in ft.

The infiltration rate of the streambed per unit area per foot of head loss varies with the temperature of the water in the stream. A decrease in the temperature of the surface water increases its viscosity and thereby decreases the infiltration rate. A decline in the temperature of surface water of one degree Fahrenheit will decrease the infiltration rate about 1.5 per cent (Rorabaugh, 1951) through the range usually encountered in practical problems. The infiltration rate for any particular surface water temperature can be computed with figure 3B and the following equation:

$$I_t = I_h \frac{\mu_a}{\mu_t} \qquad (19)$$

where: I_t = average infiltration rate of streambed for a particular surface water temperature, in gpd/acre/ft; I_h = average infiltration rate of streambed determined

from aquifer test results, in gpd/acre/ft; μ_a = coefficient of viscosity at temperature of surface water during aquifer test, in centimeter-gram-second (C.G.S.) units; and μ_t = coefficient of viscosity at a particular temperature of surface water, in C.G.S. units.

The infiltration rate also may not remain stable over a long period because of alternate sedimentation and scouring by the stream.

AQUIFER TEST DATA

The results of two aquifer tests were studied to determine the relation between the effects of induced infiltration on water levels estimated with the image-well theory and electric analog computers. The selected aquifer tests involve the two extreme aquifer-stream situations, i.e., the case where the cone of depression spreads beneath and beyond the entire streambed and the case where the cone of depression spreads only part way beneath the streambed.

Aquifer Test 1

During 1955 and 1956 an intensive hydrogeologic study was made to determine the feasibility of developing a large water-supply for the city of Springfield, Ohio, from a sand and gravel aquifer in an area along the Mad River, about 4 miles northwest of the city. The study included a test drilling program and a controlled aquifer test.

The unconsolidated deposits in the study area consist of recent silty alluvial materials and glacial outwash sand and gravel. These deposits are contained in a buried valley cut into the underlying bedrock of Ordovician and Silurian ages. The permeable outwash forming the aquifer averages about 100 feet thick and consists of permeable sand and gravel and occasional thin lenses of clayey materials. Logs of wells and test holes show that the aquifer is about 4000 feet wide and trends southwest to northeast through the study area. The Mad River has been dredged into the aquifer.

The aquifer test was made by Schaefer and Walton, Consulting Ground-Water Hydrologists, and Black and Veatch, Consulting Engineers, for the city of Springfield, Ohio, during the period February 20 through 23, 1956. A group of 6 wells on a line approximately parallel to and 400 feet west of the Mad River as shown in figure 4 was used. Pumping was at a constant rate of 1034 gpm.

Values of drawdowns adjusted for the effects of dewatering wells N-1, N-2, N-3, and N-4 at a time 4310 minutes after pumping started were plotted on semilogarithmic paper against the logarithms of distance from the pumped well, as shown in figure 5. A straight line was drawn through the points. The slope of the straight line per log cycle and the pumping rate were substituted into equation 5, and the coefficient of transmissibility was computed to be 547,000 gpd/ft.

The distance "a" from the pumped well to the recharge boundary was determined by substituting the computed value of the coefficient of transmissibility, the measured rate of pumping, and values of drawdowns in the observation wells into equation 6. The average distance "a" was found to be 686 feet.

The coefficient of storage was determined to be 0.01 by substituting the computed values of T, selected values of S and the drawdowns in the observation wells at the end of the test into equation 8. The percentage of pumped water being diverted from the Mad River was estimated to be 93 with equation 15 and figure 3A. Q_r is then equal to 960 gpm based on equation 16.

Points within the streambed up and down stream from the pumped well where drawdown was negligible were located with figure 4, the hydrogeologic properties of the aquifer, and equation 8. The reach of the streambed within the area of influence of pumping was computed to be about 8000 feet and the average width of the streambed is 82 feet. The streambed area of infiltration is, therefore, about 656,000 square feet. These values of Q_r and A_r were inserted in equation 17 and the infiltra-

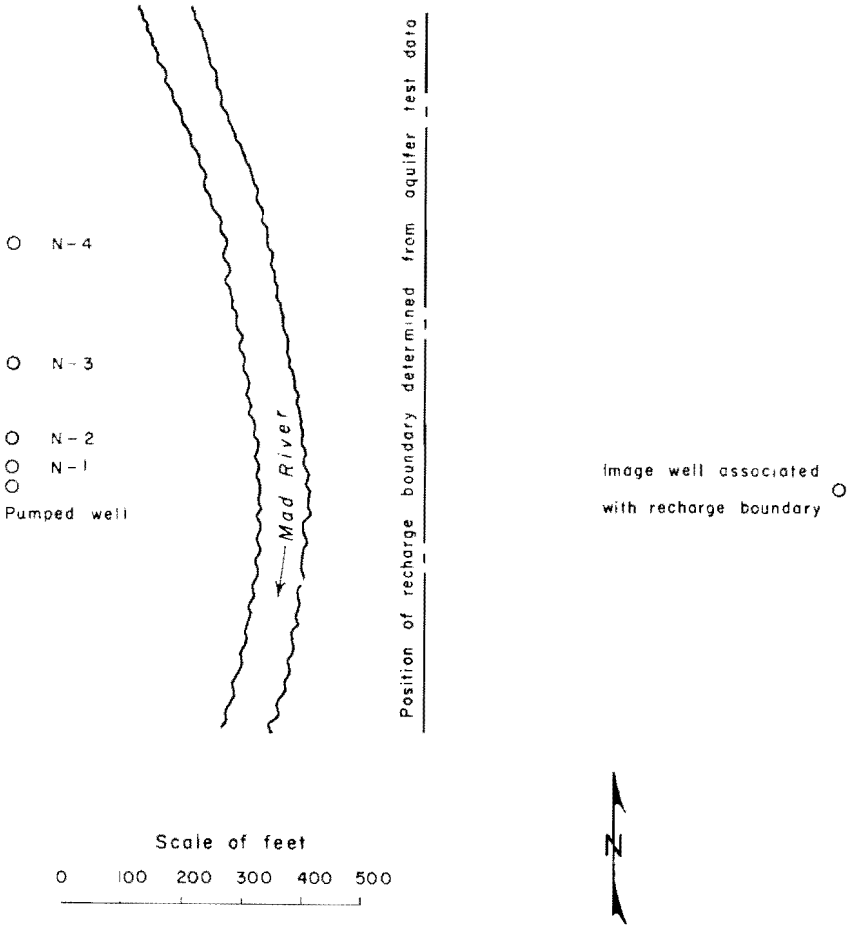

Figure 4. Location of wells used in aquifer test 1.

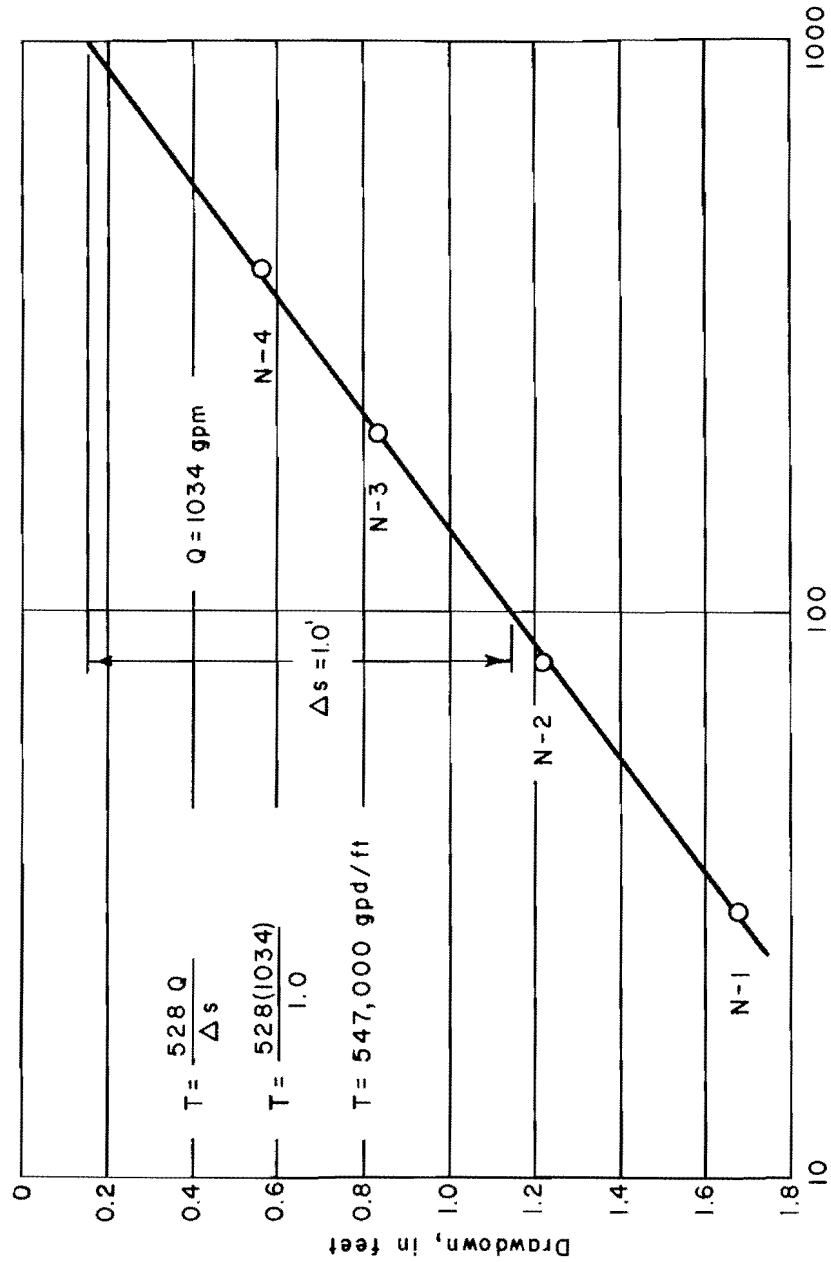

Figure 5. Semilogarithmic distance-drawdown graph for aquifer test 1.

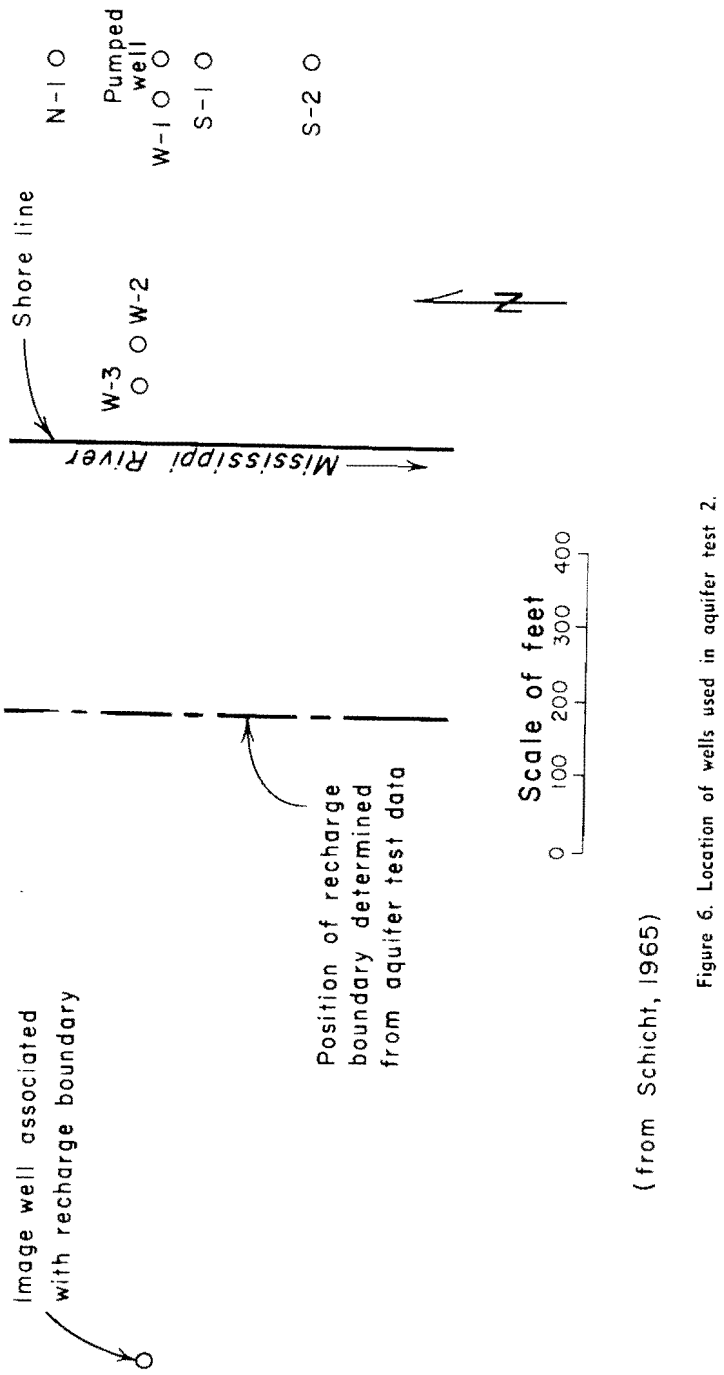

Figure 6. Location of wells used in aquifer test 2.

(from Schicht, 1965)

tion rate, l_a, was computed to be about 9.2×10^1 gpd/acre. Values of s_r were computed with equation 8, the hydrogeologic properties of the aquifer, and figure 4; the average computed value of s_r is 0.09 feet. From equation 18 the infiltration rate per foot of head loss, l_h, was found to be about 1.0×10^6 gpd/acre/ft.

Aquifer Test 2

An aquifer test was made during the period August 4 to 8, 1952, by Ranney Method Water Supplies, Incorporated, for the Monsanto Chemical Corp. (see Schicht, 1965). The test site is located east of Monsanto, Illinois, along the Mississippi River in Sec. 27, T. 2N, R. 10W. A group of seven wells, as shown in figure 6, was used. The wells were arranged in a T pattern with 4 wells parallel to and 515 feet east of the Mississippi River and 3 wells perpendicular to the river. Pumping was started at 6:00 p.m. on August 4 and was continued at a constant rate of 1100 gpm until 6:00 p.m. on August 8 when pumping was stopped and water levels were allowed to recover.

Observation wells S-1, W-1, N-1, S-2, W-2, were 7 inches in diameter and were drilled to depths of about 100 feet. The pumped well was 12 inches in diameter and was drilled to a depth of 99 feet; 10 feet of screen was installed at the bottom. Logs of wells are given in Table 1. Recording gages were installed on the observation wells; Mississippi River stages were available from St. Louis, Missouri River gage.

Values of drawdown in wells W-1 and S-2 at the end of the test were plotted on semilogarithmic paper against logarithms of distances from the pumped well, as shown in figure 7. A straight line was drawn through the points. The slope of the straight line per log cycle and the pumping rate were substituted into equation 5 and the coefficient of transmissibility was computed to be 290,000 gpd/ft.

Time-drawdown graphs were prepared for the observation wells. The nonequilibrium type curve (see Walton, 1962) was matched to the time-drawdown graphs based on the computed coefficient of transmissibility. The average coefficient of

Table 1. Driller's Logs of Wells Used in Aquifer Test 2

Formation	From (ft)	To
Well S-1		
Gray sandy clay	0	30
Gray fine sandy clay	30	40
Coarse gray sand, small gravel, 30% gravel	40	45
Gray fine sand, scattered fine gravel, brown fine sand	45	66
Brown coarse sand, fine gravel	66	76
Coarse sand and gravel	76	90
Coarse sand, fine to medium gravel	90	100
Bedrock at about 120 ft		
Well S-2		
Gray sandy clay	0	30
Gray fine sandy clay	30	40
Coarse gray sand, small gravel, 30% gravel	40	45
Gray fine sand, scattered fine gravel, brown fine sand	45	66
Brown coarse sand, fine gravel	66	75
Brown coarse sand, fine gravel, some gray clay, 40% gravel	75	76
Coarse sand, small to large gravel, 45% gravel	76	90
Brown coarse sand, fine to medium gravel, 43% gravel	90	100

(from Schicht, 1965)

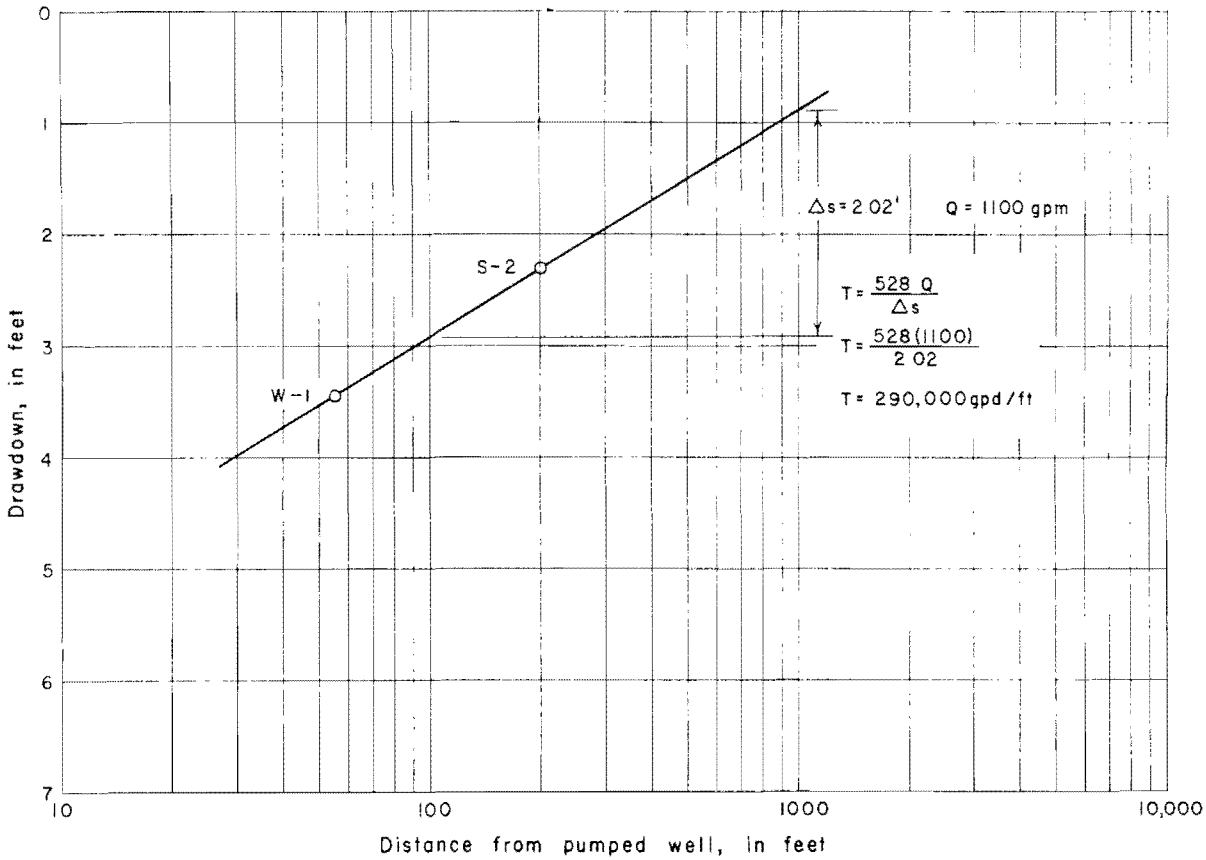

Figure 7. Semilagarithmic distance-drawdown graph for aquifer test 2.

Table 2. Summary of Aquifer Test Results

Owner of Wells	Location of test site	Date of test	Pumping period (days)	Pumping rate (gpm)	Hydrogeologic Properties						Temperature of surface water (°F)
					T (gpd/ft)	P (gpd/sq ft)	S	t_0 (gpd/acre)	s_e (ft)	h_0 (gpd/acre/ft)	
City of Springfield, Ohio	Along Mad River, about 4 miles northwest of Springfield, Ohio	2/20-23/56	3	1034	547,000	5470	0.01	92,000	0.09	1,000,000	39
The Southwestern Ohio Water Co., Cincinnati, Ohio	Along Miami River, 14 miles northwest of Cincinnati, Ohio	1954	5	1175	345,000	2760		224,000	1.33	168,000	82
City of Anderson, Indiana	Along White River, immediately upstream from the confluence of White River and Killbuck Creek at Anderson, Indiana	1953	1½	170	151,000	4720	0.05	42,000	0.20	216,000	54
City of Canton, Ohio	Along Sandy Creek, 12 miles south of Canton, Ohio	6/20-27/55	7	1020	204,000	1700	0.01	331,000	0.46	720,000	69
City of Anderson, Indiana	Along White River, 1 mile west of Anderson, Indiana, ½ mile below sewage treatment plant	1/17-22/57	4½	355	169,000	4000	0.07	52,100	1.31	39,800	35
Olin Mathison Chemical Corp.	Along Mississippi River, near East St. Louis, Illinois	2/13-17/59	4	7000	100,000	1100	0.10	418,000	1.37	305,000	33
Shell Oil Company	Along Mississippi River, near East St. Louis, Illinois	3/3-6/52	3	510	190,000	1900	0.002	9,800	0.27	35,300	38
Monsanto Chemical Corp.	Along Mississippi River, near East St. Louis, Illinois	8/4-8/52	4	1100	290,000	3900	0.08	15,500	0.17	91,200	83

storage was determined to be 0.08 with match-point coordinates. The divergences of time-drawdown curves due to the effects of the recharge boundary at the end of the test from type-curve traces were noted and the average distance "a" was computed to be 895 feet with equation 12.

The percentage of pumped water being diverted from the Mississippi River was estimated to be 46 with equation 15 and figure 3A. Q_r is then equal to 500 gpm based on equation 16.

Points within the streambed up and down stream from the pumped well where drawdown was negligible were located with figure 6, the hydrogeologic properties of the aquifer, and equation 8. The reach of the streambed within the area of influence of pumping was computed to be about 5800 feet and the average width of the streambed affected by pumping is 350 feet. The streambed area of infiltration is, therefore, about 2×10^6 square feet. Values of Q_r and A_r were inserted in equation 17, from which the infiltration rate, I_h, was computed to be about 1.55×10^4 gpd/acre. Values of s_r were estimated with equation 8, the hydrogeologic properties of the aquifer and figure 6; the average computed value of s_r is 0.17 feet. From equation 18 the infiltration rate per foot of head loss, I_h, was estimated to be about 9.1×10^4 gpd/acre/ft.

Summary of Aquifer Test Data

A summary of the aquifer-test data collected to date by the writers and the infiltration rates computed therefrom are given in table 2. Values of I_h range from 35,300 to 1,000,000 gpd/acre/ft. Fair and Geyer (1954) give infiltration rates of slow and rapid sand filters, summarized in table 3 which may be compared with infiltration rates given in table 2. Most streambeds fall into the clogged slow sand filter classification.

Table 3. Summary of Infiltration Rate Data for Slow and Rapid Sand Filters

	Slow Sand Filter	Rapid Sand Filter
Infiltration rate (I_h)	1 to 4 to 10 mgd	100 to 125 to 200 mgd
Size of bed	Large, ½ acre	Small, 1/100 to 1/10 acre
Depth of bed	12 in. of gravel; 42 in. of sand, usually reduced to 24 in. by scraping	18 in. of gravel; 30 in. of sand or less
Size of sand	Effective size 0.25 to 0.3 to 0.35 mm; uniformity coefficient 2 to 2.5 to 3	0.45 mm and higher; uniformity coefficient 1.5 and lower
Loss of head (s_r)	0.2 ft initial to 4 ft final	1 ft initial to 9 ft final
Length of run between cleaning	20 to 30 to 60 days	12 to 24 to 40 hrs
Infiltration rate (I_h)	5,000,000 to 20,000,000 gpd/acre/ft to 50,000,000 gpd/acre/ft initial 250,000 to 1,000,000 to 2,500,000 gpd/acre/ft final	100,000,000 to 125,000,000 to 200,000,000 gpd/acre/ft initial; 11,000,000 to 14,000,000 to 22,000,000 gpd/acre/ft final

ELECTRIC ANALOG COMPUTERS

Electric analog computers for the two aquifer test sites were constructed using the computed values of the coefficients of transmissibility and storage of the aquifers and infiltration rates (I_h) of the streambeds. The analog computers were patterned after analog computers developed by the U. S. Geological Survey (Skibitzke, 1961). The analog computers consist of analog models and excitation-response apparatus.

Analog Models

The analog models are regular arrays of resistors and capacitors. In the resistor-capacitor network, resistors are inversely proportional to the coefficients of transmissibility of the aquifers and the infiltration rates (I_h) of the streambeds; capacitors store electrostatic energy in a manner analogous to the storage of water within the aquifers. Electrical networks are scaled-down versions of the aquifer-stream systems.

Aquifers are continuous while a resistor-capacitor network is characterized by junctions and discrete branches. Thus, the network is only an approximation of a true analog. However, it will be shown mathematically that, if the mesh size of the network is small in comparison with the areal extent of the aquifer, the response of the network to excitation describes closely the response of an aquifer to pumping.

Suppose the area of an aquifer is subdivided into squares of equal area and sides of length "b" as shown in Figure 8A. The intersections of the grid lines are called nodes and are numbered. The area of the squares, b^2, is very small in comparison to the areal extent of the aquifer. Consider a resistor-capacitor network with a square pattern as shown in Figure 8A and network junctions at nodes as defined in Figure 8B. The junctions consist of 4 equal valued resistors and 1 capacitor connected to a common terminal; the capacitor is also connected to ground.

With reference to Figure 8A, the finite-difference form of the partial differential equation governing the nonsteady state, two-dimensional flow of ground water in a homogeneous, isotropic, artesian aquifer infinite in areal extent may be written in abbreviated form as (see Stallman, 1956):

$$T\left(\sum_{2}^{5} h_i - 4h_1\right) = b^2 S \frac{\partial h_1}{\partial t} \qquad (20)$$

where: h_1 is the head at node 1; h_i, i equals 2, 3, 4 and 5, represents heads at nodes 2 to 5; b is the width of the grid interval; t is time; T is the coefficient of transmissibility; and S is the coefficient of storage.

The relation of electrical potentials in the vicinity of the junction in Figure 8B can be expressed in abbreviated form as (see Stallman, 1961 and Millman and Seely, 1941):

$$\frac{1}{R}\left(\sum_{2}^{5} V_i - 4V_1\right) = C \frac{\partial V}{\partial t} \qquad (21)$$

where: V_i, i equals 2, 3, 4 and 5, is the electrical potential at ends of resistors A to D; t is time; R is the resistance; and C is the capacitance.

Comparison of equations 20 and 21 shows the equation governing the flow of water in an aquifer is of the same form as the equation governing the flow of

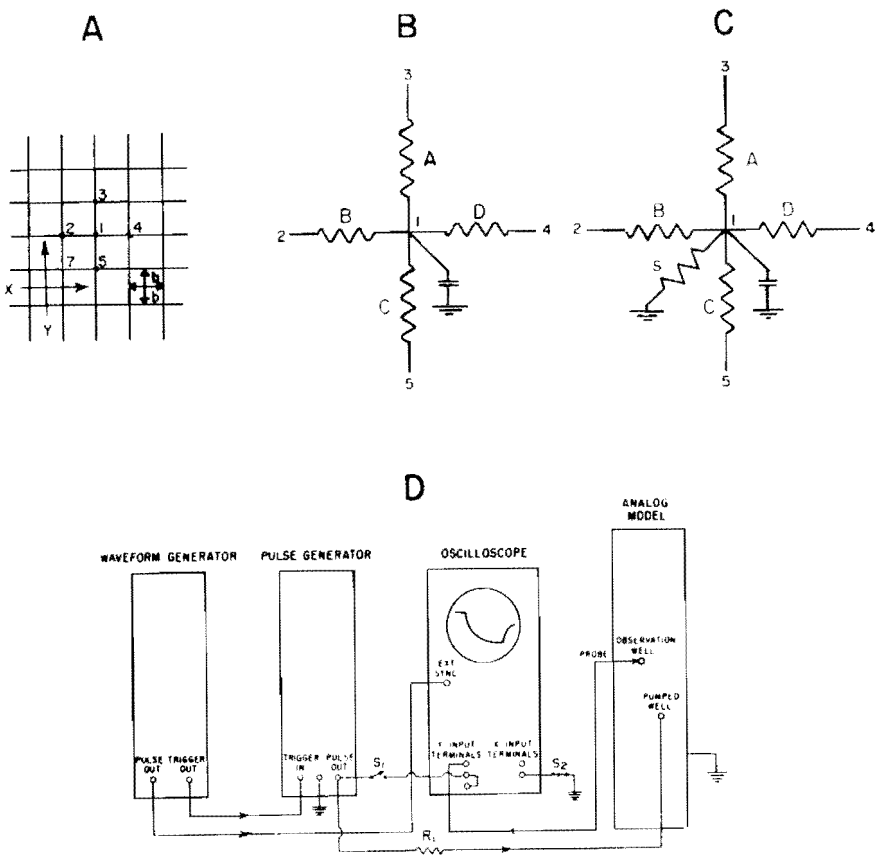

Figure 8. Finite-difference grid (A), resistor-capacitor nets (B and C) and block diagram describing analog computer components (D).

electrical current in the prescribed resistor-capacitor network. For every term in equation 20 there is a corresponding term of the same order of differentiation in equation 21. Thus, the analogy between electrical systems and aquifer systems is apparent. The hydraulic heads, h, are analogous to electrical potentials, V. The coefficient of transmissibility, T, is analogous to the reciprocal of the electrical resistance, 1/R. The product of the coefficient of storage, S, and b^2 is analogous to the electrical capacitance, C. Continuing the comparison, water moves in an aquifer in a manner similar to the way charges move in an electrical circuit. The quantity of water is calculated in gallons while the charge is calculated in coulombs. The rate of flow of water past a point in the aquifer is expressed in gallons per day, while the flow of electricity is expressed in coulombs per second, or amperes. The hydraulic head loss between two points in an aquifer is expressed in feet, while the potential drop across a part of the electrical circuit is in volts.

There are four scale factors connecting units in the hydraulic system to the analogous units in the electrical system. The four scale factors are defined by the following equations (Bermes, 1960):

$$q = K_1 Q \tag{22}$$

$$h = K_2 V \tag{23}$$

$$Q = K_3 I \tag{24}$$

$$t_d = K_4 t_s \tag{25}$$

where: q is in gallons, Q is in coulombs, h is in ft, V is in volts, Q is in gallons per day, I is in amps, t_d is in days, t_s is in seconds, K_1 is in gallons per coulomb, K_2 is in ft per volt, K_3 is in gallons per day per amp, and K_4 is in days per second. The relation between scale factors K_1, K_3 and K_4 is expressed by the following equation:

$$\frac{K_3 K_4}{K_1} = 1 \tag{26}$$

The following equations derived from equations 23 and 24 may be used to compute values of resistors and capacitors in the interior portions of the analog model (Walton and Prickett, 1963):

$$R = \frac{K_3}{K_2 T} \tag{27}$$

$$C = 7.48\ b^2 S\ \frac{K_2}{K_1} \tag{28}$$

where: R is in ohms, T is in gallons per day per foot (gpd/ft), C is in farads, S is a fraction, and b is in ft. To minimize computer costs, scale factors are chosen that allow the use of standard tolerance, low voltage, fixed carbon resistors generally with values from 10^2 ohms to 10^7 ohms, and capacitors of low voltage rating with values from 10^1 $\mu\mu$f to 10^5 $\mu\mu$f.

The values of resistors and capacitors adjacent to boundaries can be computed based on the "vector area" technique described by Karplus (1958). Variation in net spacing also can be accomplished with techniques described by Karplus (1958).

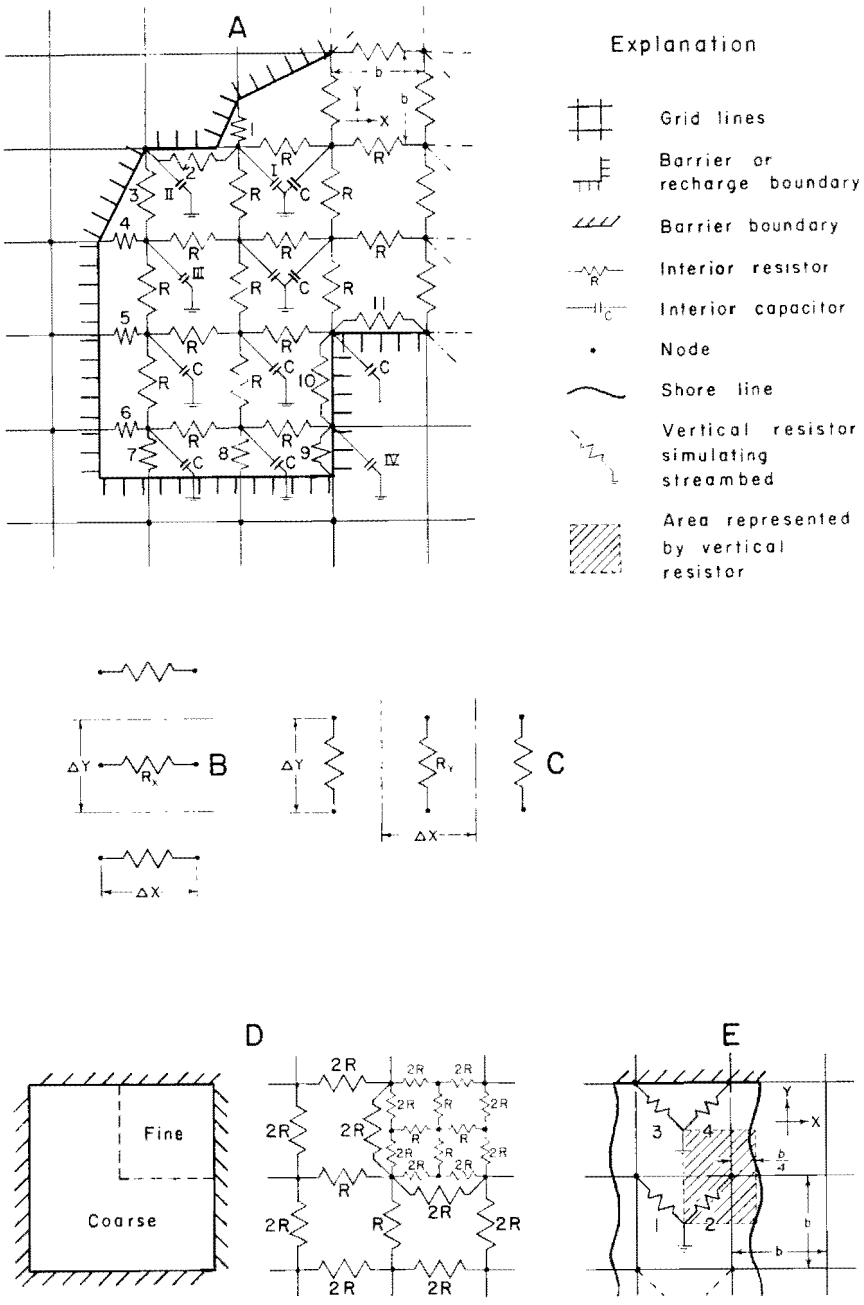

Figure 9. Vector area techniques for computing values of resistors and capacitors adjacent to boundaries.

The following equations (see Karplus, 1958) may be used to compute values of resistors adjacent to boundaries:

$$R_x = R\,\frac{\Delta X}{\Delta Y} \tag{29}$$

$$R_y = R\,\frac{\Delta Y}{\Delta X} \tag{30}$$

where: R_x is the value of the x-direction resistor adjacent to a boundary, in ohms; R_y is the value of the y-direction resistor adjacent to a boundary in ohms; R is the value of resistors in interior portions of the model, in ohms; X is the X dimension of the portion of the aquifer represented by the resistor, in ft; and Y is the Y dimension of the portion of the aquifer represented by the resistor, in ft.

Suppose that a barrier or recharge boundary does not coincide with the lines of part of the grid as shown in figure 9A. The vector areas corresponding to R_5 and R_6 have the same width ΔY (see figure 9B) as those of interior resistors R, and a length of $0.5\Delta X$ (see figure 9B) so that from equation 29, $R_5 = R_6 = 0.5R$. The vector areas corresponding to R_7 and R_8 have the same width ΔX (see figure 9C) as those of the interior resistors R, but a length of $0.5\Delta Y$ (see figure 9C), so that from equation 30, $R_7 = R_8 = 0.5R_{10}$. The vector area corresponding to R_1 has an average width (ΔY) of $0.9\Delta Y$ compared to an interior resistor R and an average length (ΔX) of $0.45\Delta X$ compared to an interior resistor R, so that from equation 29, $R_1 = 0.5R$.

Suppose that a barrier or recharge boundary coincides with the lines of part of the grid as shown in figure 9A. The vector area corresponding to R_{11} has the same length ΔX (see figure 9B) as an interior resistor R, but a width of $0.5\Delta Y$ (see figure 9B) so that from equation 29, $R_{11} = 2R$. The vector area corresponding to R_{10} has the same length ΔY (see figure 9C) as an interior resistor R, but a width of $0.5\Delta X$ (see figure 9C) so that from equation 30, $R_{10} = 2R$. The vector area corresponding to R_9 has a length of $0.5\Delta Y$ (see figure 9C) compared to an interior resistor R, and a width of $0.5\Delta X$ (see figure 9C) so that from equation 30, $R_{10} = R$.

Values of resistors in figure 9A are $R_1 = 1.1R$, $R_2 = 1.9R$, $R_3 = 1.5R$, $R_4 = 0.5R$, $R_5 = 0.5R$, $R_6 = 0.5R$, $R_7 = 0.5R$, $R_8 = 0.5R$, $R_9 = R$, $R_{10} = 2R$ and $R_{11} = 2R$.

In order to obtain satisfactory solutions to ground-water flow problems with a minimum number of electrical components, it is often advantageous to employ coarse grids in some sections of the model and fine grids in other sections. A simple method for effecting a variation in net spacing is to regard the "coarse" and "fine" sections as separate portions of the model and to treat the interface between the two sections as a barrier boundary (Karplus, 1958). The two grids are then jointed at appropriate nodes. Figure 9D illustrates how a variation in the ratio of 1:2 may be accomplished.

The magnitude of resistors (R_s) simulating the streambed are inversely proportional to the areas of the portions of the streambed they represent. The following equation derived by substituting Ohm's and Darcy's laws into equation 24, may be used to compute the values of resistors simulating the streambed:

$$R_s = \frac{K_3}{K_2(I_h)A_s} \tag{31}$$

where: A_s is the area of the streambed represented by the resistor, in sq ft.

The vector areas (A_s) corresponding to R_{s1} and R_{s2} in figure 9E are $\frac{3}{4}b^2$ ($\frac{3}{4}b \times b$), thus, $R_{s1} = R_{s2} = K_3/K_2(I_h)\frac{3}{4}b^2$. The vector areas ($A_s$) corresponding to R_{s3} and R_{s4} in figure 9E are $\frac{3}{8}b^2$ ($\frac{3}{4}b \times \frac{1}{2}b$), thus, $R_{s3} = R_{s4} = K_3/K_2(I_h)\frac{3}{8}b^2$.

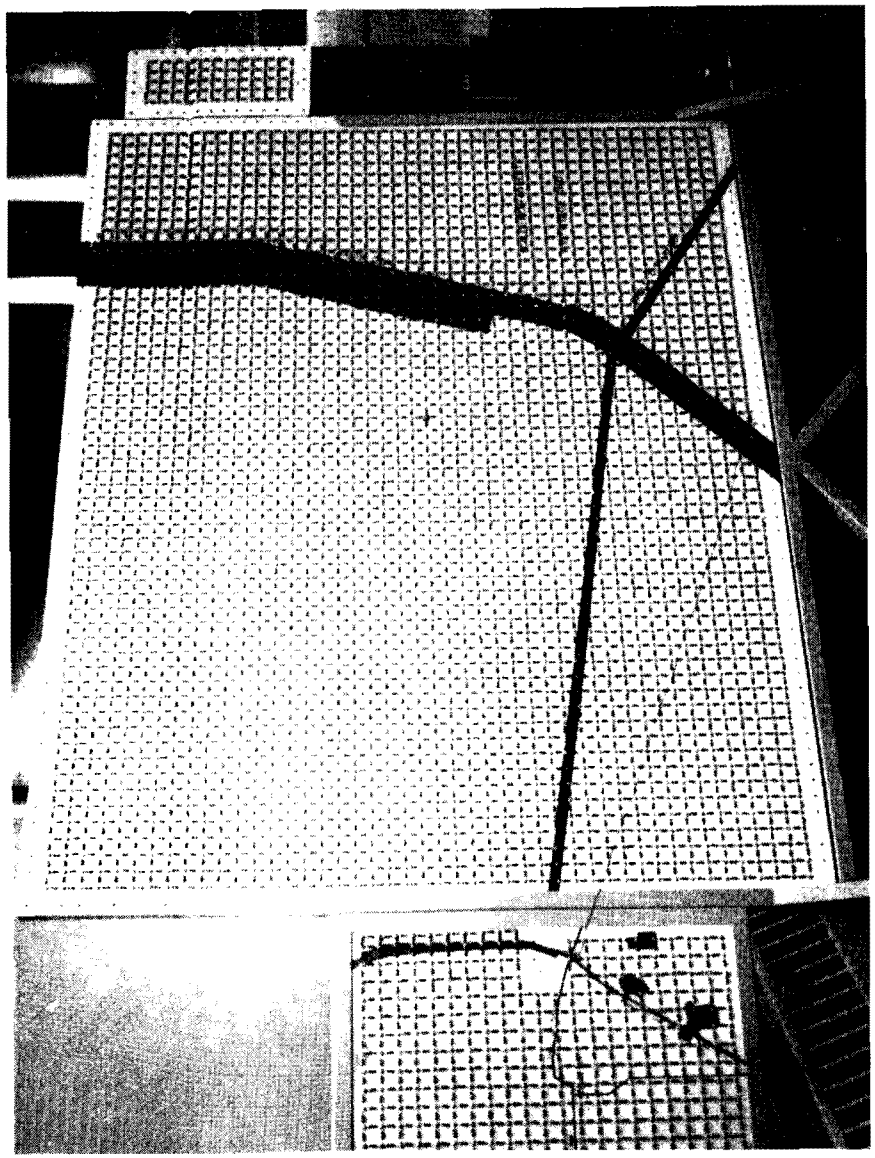

Figure 10. Analog model for aquifer test site 1.

The magnitudes of capacitors are directly proportional to the areas of the portions of the aquifer they represent. The values of the capacitors (C_b) adjacent to boundaries may be computed with the following equation:

$$C_b = 7.48\ A_c\ S\ \frac{K_2}{K_1} \tag{32}$$

where: A_c is the area of the aquifer represented by the capacitor, in sq ft.

The vector area corresponding to C_{III} (see figure 9A) is $0.94b^2$, so that $C_{III} = 0.94C_a$. Values of capacitors in figure 9A are $C_I = 0.80C$, $C_{II} = 0.38C$, $C_{III} = 0.94C$ and $C_{IV} = 0.25C$.

The analog model for aquifer test site 1 consists of regular arrays of 6,100 resistors and 3,100 capacitors and is shown in figure 10. The values of resistors range from 1.2×10^1 to 5.6×10^6 ohms and the values of capacitors range from 5 micro-micro farads to 4×10^{-3} micro farads. The fine grid of the model is 5 feet by four feet and has a scale of 1″ = 40 feet; the coarse grid of the model is 1 foot by 2 feet and has a scale of 1″ = 800 feet. Scale factors are: $K_1 = 1.19 \times 10^{13}$ gals/coulomb, $K_2 = 1$ ft/volt, $K_3 = 5.47 \times 10^{10}$ gpd/amp and $K_4 = 2.18 \times 10^2$ days/sec.

The analog model for aquifer test site 2 consists of regular arrays of 2,150 resistors and 1,060 capacitors and is shown in figure 11. The values of resistors range from 4.7×10^1 to 1.0×10^6 ohms and the values of capacitors range from 5.0×10^2 micro-micro farads to 1×10^{-2} micro farads. The model is 3 feet by 4 feet. The fine grid of the model has a scale of 1″ = 150 feet; the coarse grid of the model has a scale of 1″ = 450 feet. Scale factors are: $K_1 = 1.38 \times 10^{13}$ gals/coulomb, $K_2 = 1$ ft/volt, $K_3 = 2.1 \times 10^{10}$ gpd/amp and $K_4 = 6.58 \times 10^2$ days/sec.

The analog models were constructed with ⅛-inch pegboard perforated with holes on a 1-inch square pattern. Aluminum angles (1×1 inch) were attached along the edges of the models with metal screws. Shoe eyelets were inserted in the holes of the pegboard to provide terminals for resistors and capacitors. Horizontal arrays of resistors and capacitors simulate aquifers and vertical arrays of resistors simulate streambeds.

Excitation-Response Apparatus

Excitation-response apparatus force electrical energy in the proper time phase into the analog model and measure energy levels within the energy-dissipative resistor-capacitor network. The excitation-response apparatus consists of a power supply, waveform generator, a pulse generator and an oscilloscope as shown in figure 8D. The waveform generator, which produces sawtooth pulses, is connected to the trigger circuits of the pulse generator and the oscilloscope, thereby controlling the repetition rate of computation and synchronizing the oscilloscope's horizontal sweep and the output of the pulse generator. The pulse generator, which produces rectangular shaped pulses whose duration is analogous to the pumping period and whose amplitude is analogous to the pumping rate, is coupled to that junction in the analog model representing the pumped well. The oscilloscope is connected to junctions of the analog model representing observation wells. An electron beam is swept across the cathode ray tube of the oscilloscope providing a time-voltage graph which is analogous to the time-drawdown graph for an observation well. A means of computing the pumping rate is incorporated in the circuit between the pulse generator and the analog model by the small resistor, R_1, in series (see figure 8D). The voltage drop across the calibrated resistor is measured with the oscilloscope

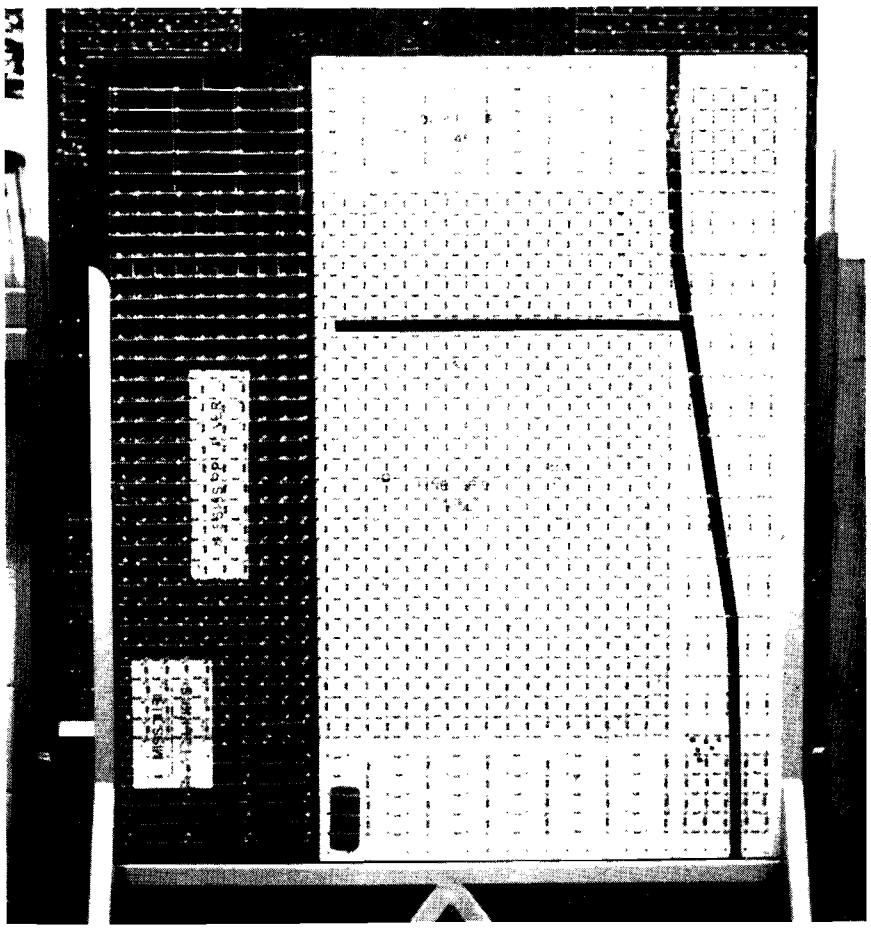

Figure 11. Analog model for aquifer test site 2.

using switches, S_1 and S_2. The voltage drop and the following equation are used to determine the pumping rate:

$$Q = \frac{V_R \, K_R}{1.44 \times 10^3 \, R_i}$$

where: Q is the pumping rate, in gpm; V_R is the voltage drop across the calibrated resistor R_i, in volts; and R_i is the calibrated resistance, in ohms.

The time-voltage graphs obtained from the oscilloscope are converted into time-drawdown graphs with equations 23 and 25. A catalog of time-drawdown graphs provides data for the construction of a series of water-level change contour maps.

The excitation-response apparatus used in this investigation is shown in figure 12 and consists of a Power Supply, a Waveform Generator, a Pulse Generator and an Oscilloscope with a Dual Trace Amplifier and a Time Base.

Results of Analog Computer Studies

The analog models were separately coupled by Gordon Grundeen, Laboratory Technician to the excitation-response apparatus and the pulse generator was connected to junctions at the locations of production wells used during aquifer tests 1 and 2. The output of the pulse generator was adjusted in accordance with the aquifer test pumping rates and periods. The oscilloscope was connected to terminals representing observation wells and water-level declines were computed from time-voltage graphs. Thus, water-level declines everywhere in the aquifers were described.

The drawdown contours for aquifer test 1 (pumping period 4310 minutes and pumping rate 1034 gpm) based on the analog computer solution are shown in figure 13. The drawdown contours for the same pumping period and rate computed with the results of aquifer test 1 and based on an analytical solution involving the image-well theory are shown in figure 14. Water-level decline hydrographs for selected observation points shown in figure 15 show that with increasing distance from the stream, drawdown decreases and the time lag of measurable drawdowns increases.

The drawdown contours for aquifer test 2 (pumping period 4 days and pumping rate 1100 gpm) based on the analog computer solution are shown in figure 16. The drawdown contours for the same pumping period and rate computed with the results of aquifer test 2 and based on an analytical solution involving the image well theory are given in figure 17. Water-level decline hydrographs for selected observation points are shown in figures 18 and 19.

In the case of aquifer test 1, close agreement between analog and analytical drawdown contours on the land side of the river is noted if the irregular course of the river is taken into consideration. Differences in individual drawdowns at observation points west of the river based on analog computer and analytical solutions are small. Analog and analytical drawdown contour solutions beneath the river and east of the river differ appreciably. According to the analog computer solution, the cone of depression spread a much greater distance beyond the river than suggested by the analytical solution. Also, as indicated in table 4, the I_s and s_i values based on analog computer and analytical solutions do not agree. The analog computer solution indicates that the streambed area of infiltration is greater but the average head loss is less than suggested by the analytical solution.

In the case of aquifer test 2, close agreement between analog and analytical drawdown contours on the land side of the river is noted. Differences in individual drawdowns at observation points east of the river based on analog computer and analytical solutions are small. Analog and analytical drawdown contours beneath the river differ appreciably. According to the analog computer solution, the cone

Table 4. Analog Computer and Analytical Solutions of I_a, s_r and I_h

	I_a (gpd/acre)	s_r (ft)	I_h (gpd/acre/ft)
Aquifer Test 1			
Analog Computer Solution	6.50×10^{4}	0.065	1×10^{6}
Analytical Solution	9.20×10^{4}	0.090	1×10^{6}
Aquifer Test 2			
Analog Computer Solution	6.50×10^{3}	0.072	9.1×10^{4}
Analytical Solution	1.55×10^{4}	0.170	9.1×10^{4}

of depression spread a much greater distance beyond the shore line than suggested by the analytical solution and the effective line of recharge is curved. Also, as indicated in table 4, the I_a and s_r values based on analog computer and analytical solutions do not agree. The analog computer solution indicates that the streambed area of infiltration is greater but the average head loss is less than suggested by the analytical solution.

The analog model for aquifer test site 1 was coupled by Gordon Grundeen, Laboratory Technician to a Waveform Synthesizer with a Variable Width Plug-In Unit (variable function generator) and an Oscilloscope with a Dual Trace Amplifier and a Time Base (see figure 12). The output of the variable function generator was adjusted in accordance with a selected small stream rise (figure 20) recorded for the Mad River. The variable function generator was connected to the vertical resistors simulating the streambed; the vertical resistors were disconnected from ground. The oscilloscope was connected to terminals representing observation points and water-level rises caused by the complex stream stage rise were computed from time-voltage graphs.

The water-level rise contours representing the maximum effects of the stream stage rise are shown in figure 21. Water-level rises varied from 1.75 feet beneath the streambed to 0.20 foot about 1½ miles west of the river due to the 2.0-foot stream stage rise. Approximately 15.5 million gallons of water percolated through the streambed and into temporary storage within the aquifer during the 1¼-day period of the stream-stage rise. The average rate of recharge (bank storage) was about 3.7 million gallons per day per mile length of streambed. Approximately 2.6 million gallons or 17 per cent of the recharge remained in storage within the aquifer 3¾ days after the stream-stage peak even though the stream stage had returned to its original stage. Thus, about 12.9 million gallons or 83 per cent of recharge returned to the stream during the 3¾-day period following the peak. Cooper and Rorabaugh (1963) present an excellent discussion of changes in ground-water heads, ground-water flow and bank storage resulting from a stream-stage oscillation. The water-level hydrographs for selected observation points shown in figure 20 show that with increasing distance from the stream, the water-level rise decreases and the time lag of the maximum water-level rise increases.

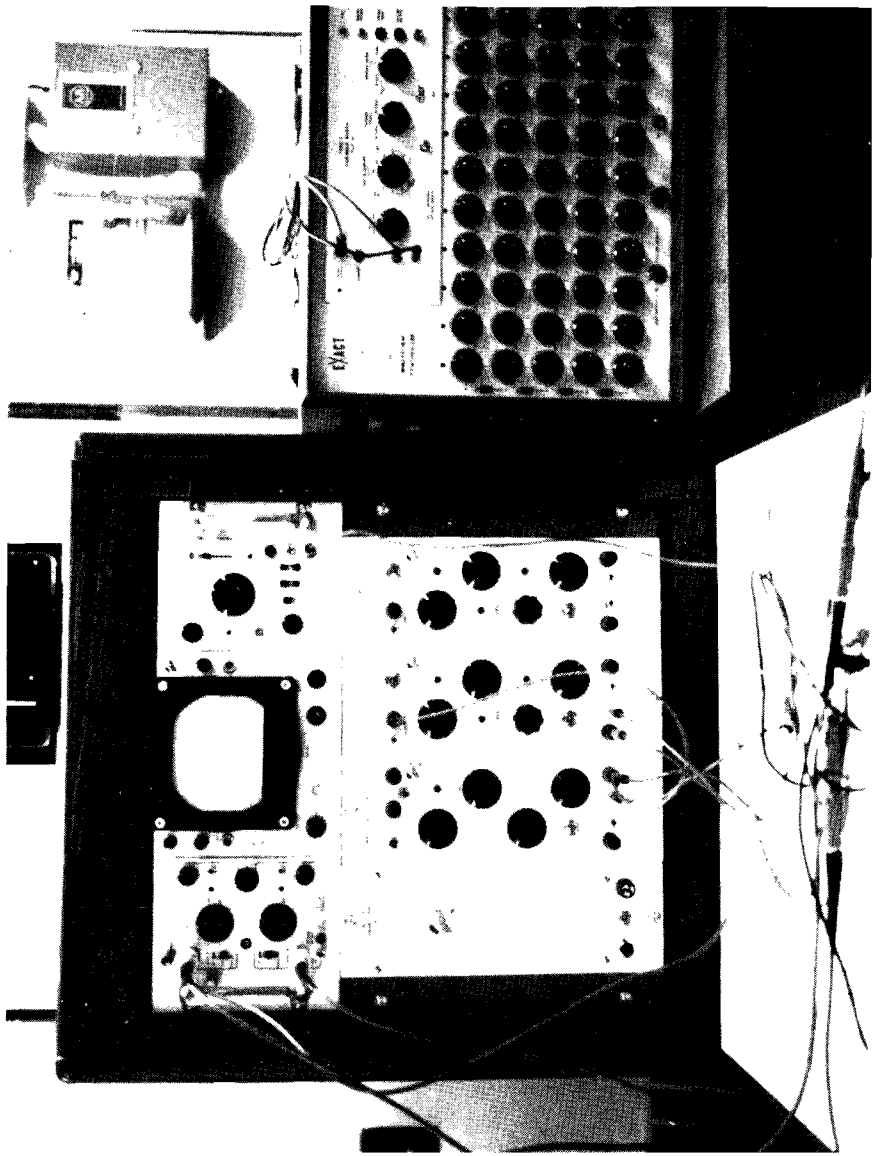

Figure 12. Excitation-response apparatus.

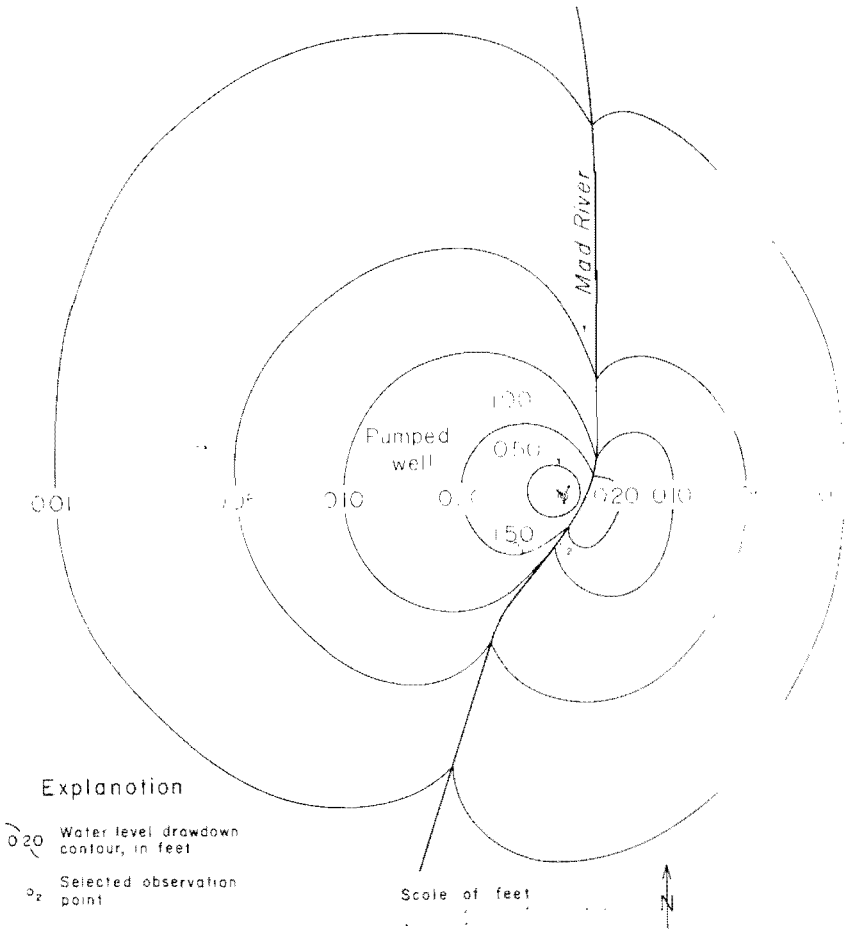

Figure 13. Drawdown contours for aquifer test 1 based on analog computer solution.

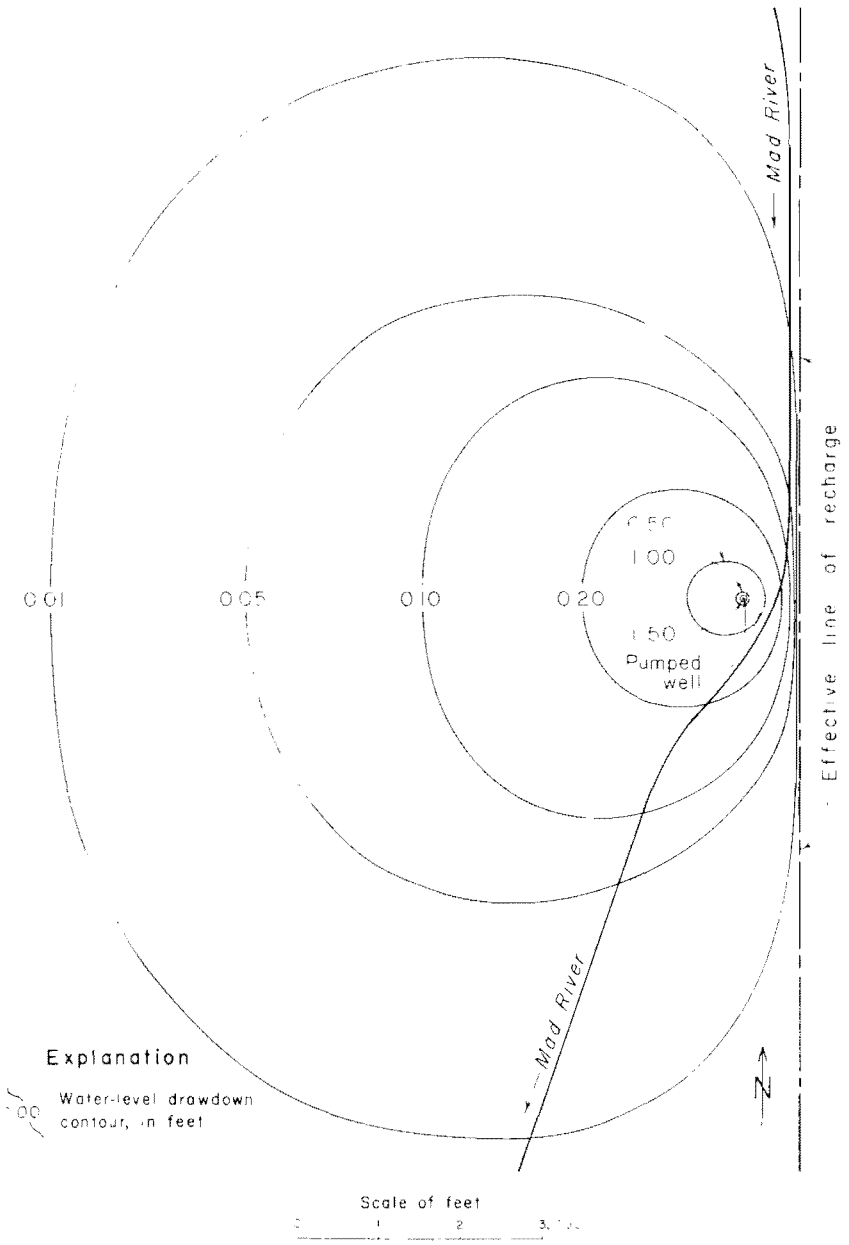

Figure 14. Drawdown contours for aquifer test 1 based on analytical solution.

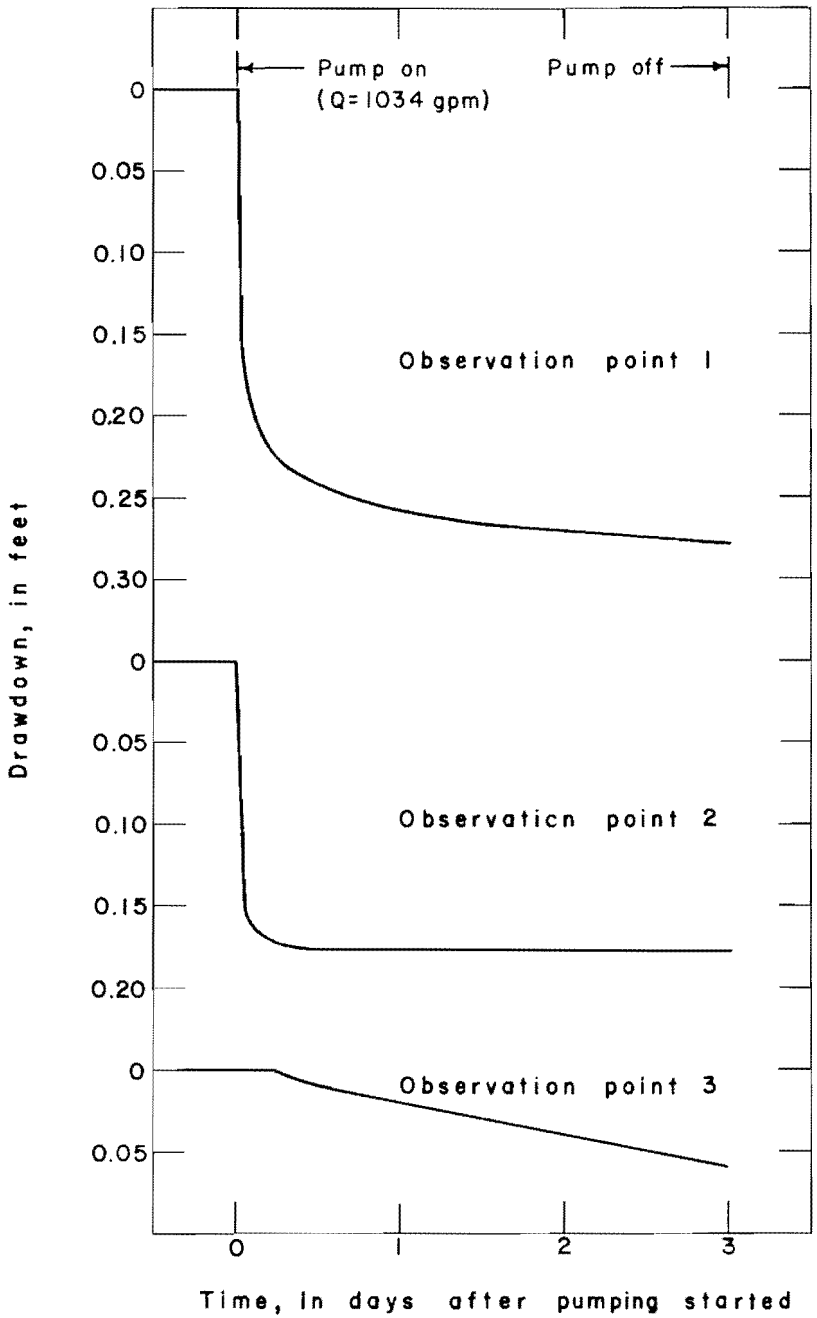

(location of observation points shown in figure 13)

Figure 15. Water-level declines at selected observation points during aquifer test 1 based on analog computer solution.

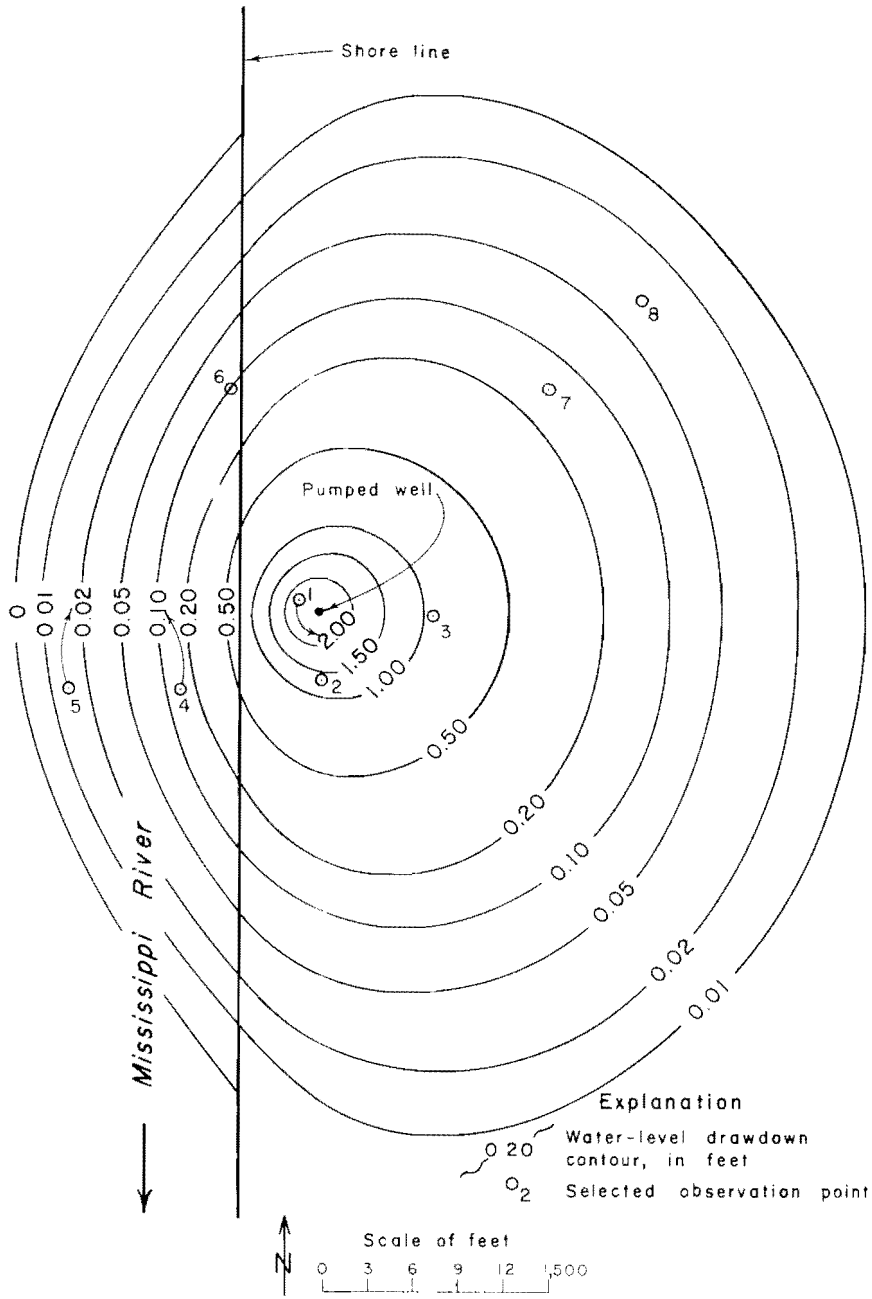

Figure 16. Drawdown contours for aquifer test 2 based on analog computer solution.

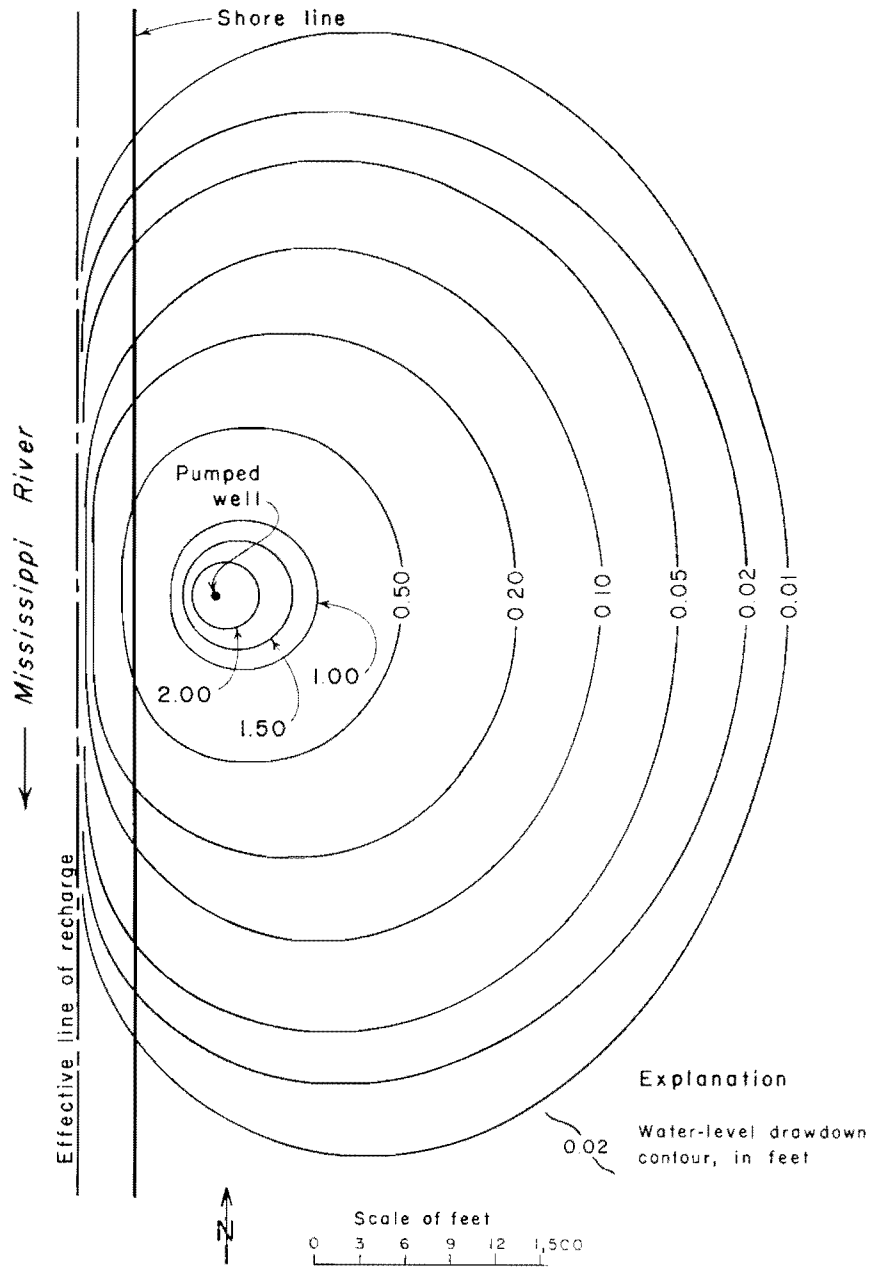

Figure 17. Drawdown contours for aquifer test 2 based on analytical solution.

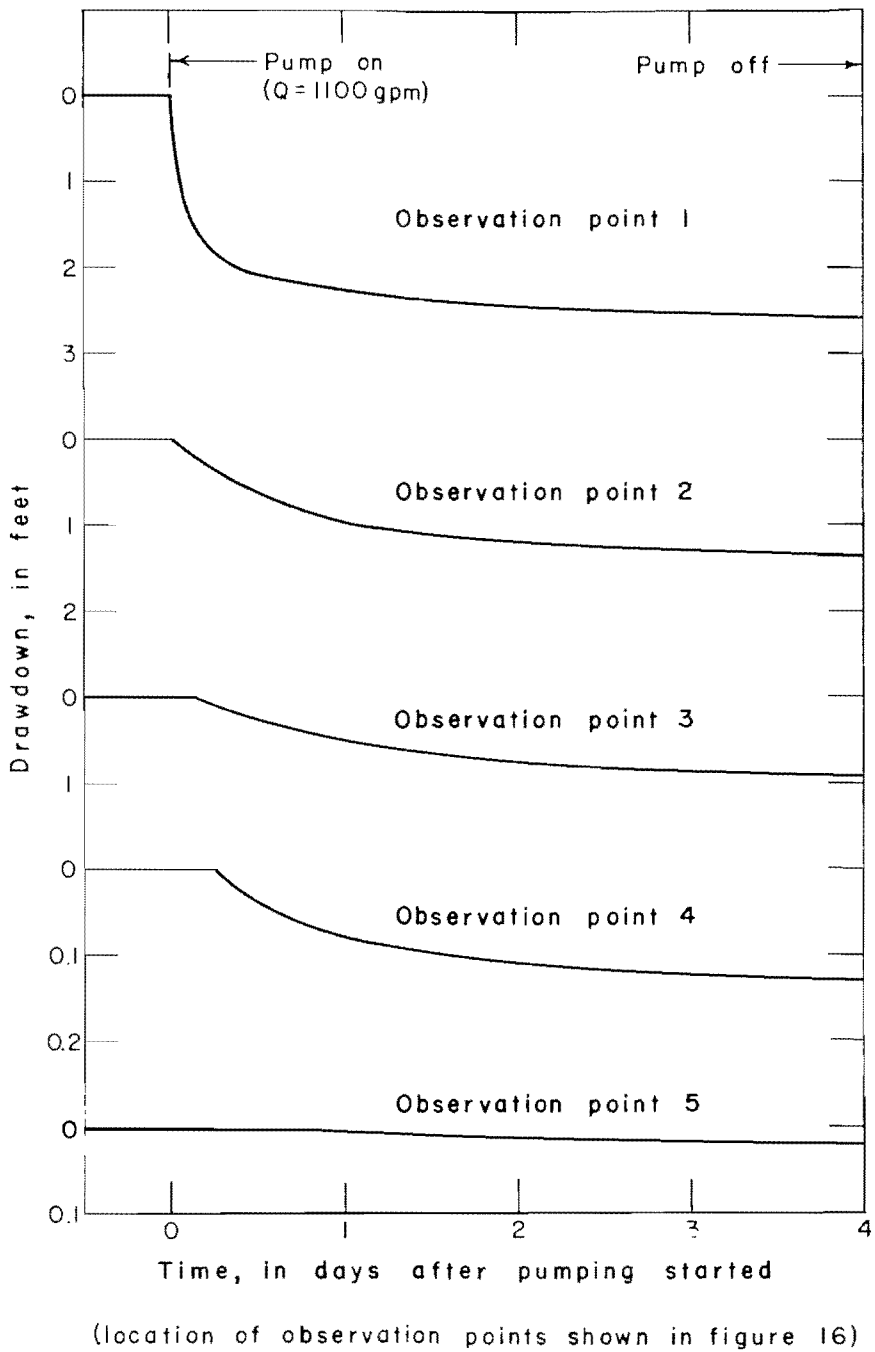

(location of observation points shown in figure 16)

Figure 18. Water-level declines at selected observation points 1-5 during aquifer test 2 based on analog solution.

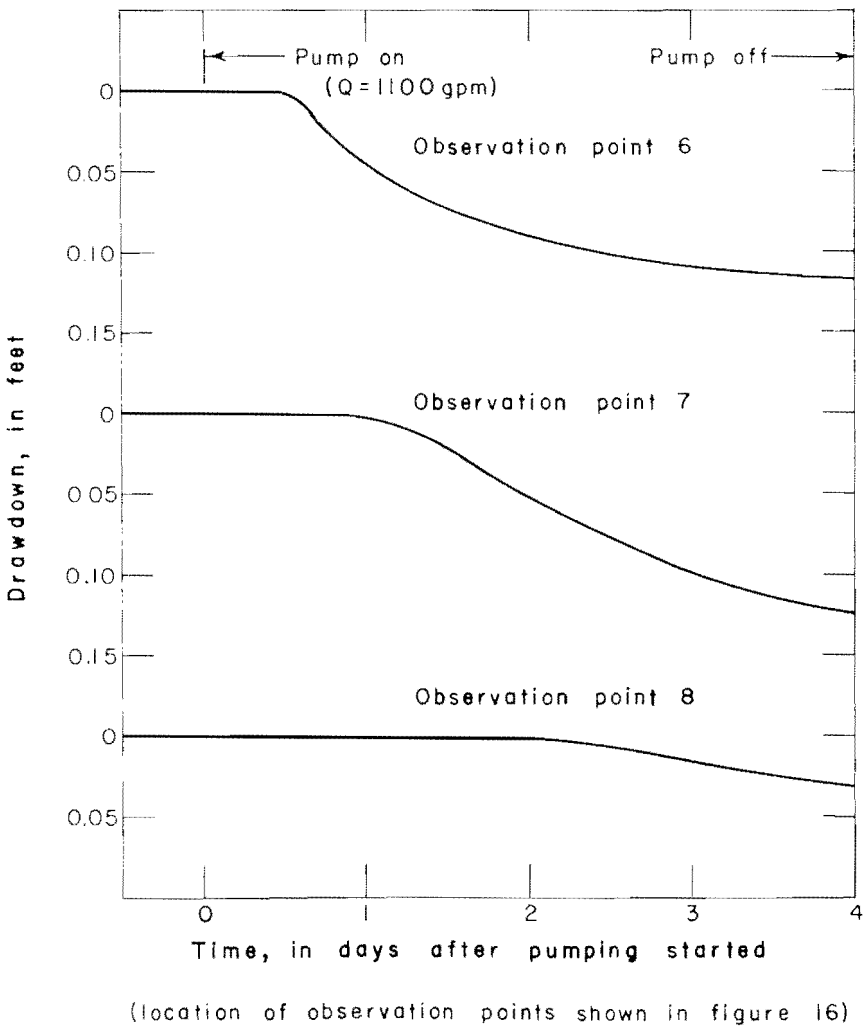

(location of observation points shown in figure 16)

Figure 19. Water-level declines at selected observation points 6-8 during aquifer test 2 based on analog solution.

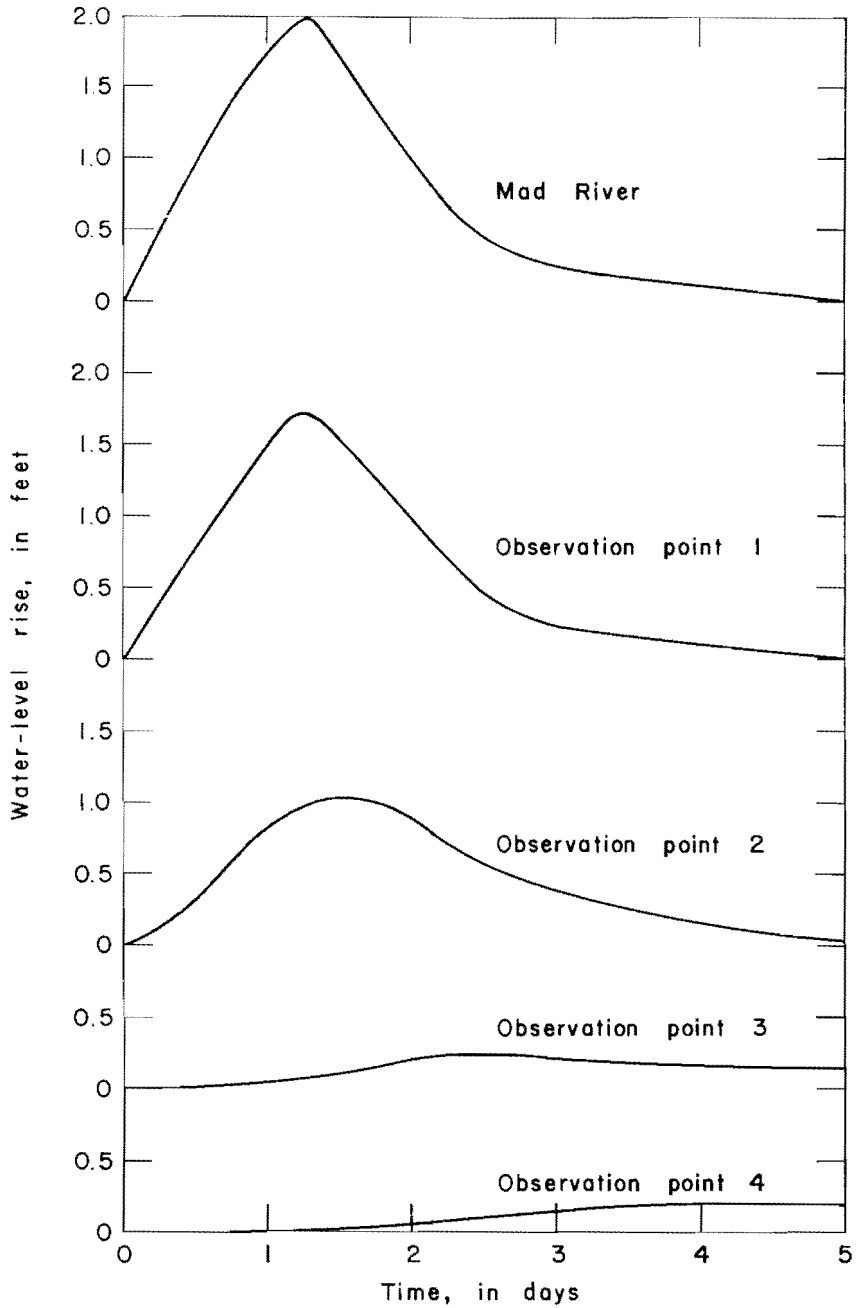

(location of observation points shown in figure 21)

Figure 20. Water-level rises at observation points due to a selected stream stage rise at aquifer test site 1.

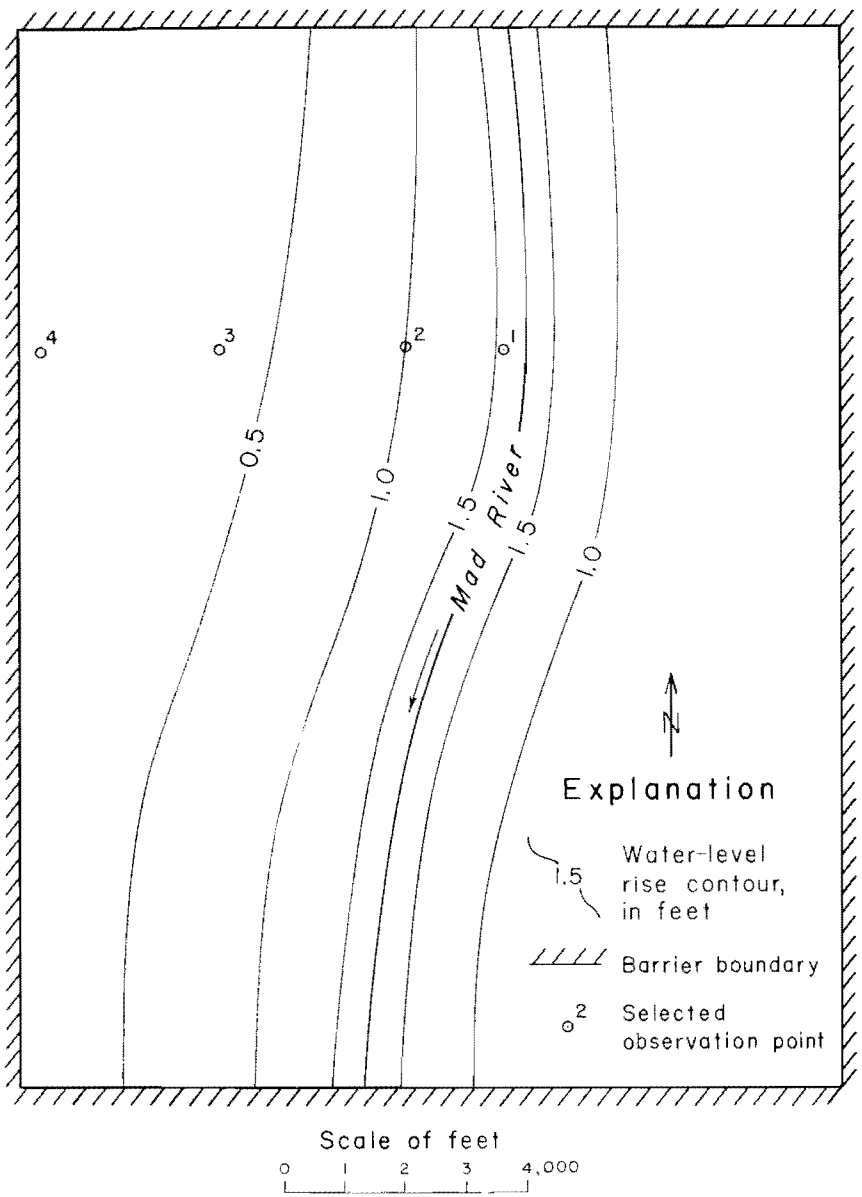

Figure 21. Water-level rise contours for a selected stream stage rise at aquifer test site 1.

CONCLUSIONS

During induced infiltration aquifer tests, the image-well theory closely describes drawdowns on the land side of the streams with a high degree of accuracy, whether the cone of depression spreads beneath and beyond or only part way beneath the streambeds. Drawdowns beneath or beyond the streambeds and the streambed areas of infiltration based on the image-well theory are not those which would be observed in the field. Analog computer studies indicate that the streambed areas of infiltration are greater but the average head losses beneath the streambeds are less than suggested by analytical solutions. Thus, it would appear that analytical methods involving the image-well theory can be used to estimate streambed infiltration rates per unit area per foot of head loss. The streambeds may be narrow or wide and have high or low permeabilities. The image-well theory may also be used to estimate drawdowns in wells on the land side of the river. However, analytical methods cannot be used to estimate streambed areas of infiltration and drawdowns beneath and beyond streambeds which would occur as the result of pumping a well adjacent to a stream.

In the past, little if any attention has been given water-level declines beneath and beyond streambeds. During future aquifer tests, observation wells should be installed within the streambeds at depths just below the streambed so that the average head losses due to the vertical percolation of water through the streambeds and the streambed areas of infiltration can be estimated.

Ground-water mathematicians are urged to conduct research which will lead to the derivation of equations relating water-level changes during aquifer tests and induced infiltration associated with a streambed having a finite width and only partially penetrating an aquifer. Streambeds in many cases may be treated as infinite strip aquitards.

Before the ground-water resources of aquifers recharged by induced infiltration of water in streams can be appraised, induced infiltration rates under varying stream-stage and aquifer water-level conditions must be evaluated. Potential recharge by the induced infiltration of surface water can be estimated from streambed infiltration rates, surface water temperatures, ground-water levels, and stream-stage data. Recharge by induced infiltration is directly proportional to the drawdown immediately below the streambed and is at a maximum when the water table is immediately below the streambed. Infiltration cannot exceed streamflow. The fact that the average depth of water in a stream will decrease as the result of induced infiltration must be considered in estimating potential recharge. Provided the water table remains below the streambed, the least amounts of induced infiltration occur during extended dry periods when streamflow and the temperature of the surface water is low.

At high pumping rates water may be withdrawn at a rate in excess of the ability of the streambed to transmit it, and as a result the water table may decline below portions of the streambed. In such a case, maximum infiltration occurs in the reach of the stream in the immediate vicinity of the pumped well, and the cone of depression spreads further up and down stream. In areas where the water table is below the streambed, induced infiltration is directly proportional to the average depth of water in the stream. In other areas, induced infiltration is directly proportional to the average difference between the water surface of the stream and the position of the water table.

Research with an electric analog computer should be conducted to investigate the factors affecting the potential recharge from streamflow under heavy pumping and variable stream-stage conditions. An aquifer-stream system could be simulated

with a regular array of resistors, capacitors, diodes, and other electric components. The stream-stage changes could be simulated with an arbitrary function generator and associated accessories. The response of the aquifer to recharge could be measured with an oscilloscope and associated accessories. Induced infiltration, especially under flood flow hydrographs, could be evaluated to determine the time and space effects of changing stream stages on recharge. The research would provide a better understanding of the role of streams in ground-water recharge.

REFERENCES

BERMES, B. J. 1960. An electric analog method for use in quantitative studies. U. S. Geological Survey mimeo. rept.

COOPER, H. H. and M. I. ROBABAUGH. 1963. Ground-water movements and bank storage due to flood stages in surface streams. U. S. Geol. Survey Water-Supply Paper 1536-J.

DARCY, HENRI. 1856. Les fontaines publiques de la Ville de Dijon. Dalmont, Paris.

FAIR, G. M., and J. C. GEYER. 1954. Water Supply and waste-water disposal: John Wiley & Sons, Inc., New York.

FOLEY, F. C., W. C. WALTON, and W. J. DRESCHER. 1953. Ground-water conditions in the Milwaukee-Waukesha area, Wisconsin. U. S. Geol. Survey Water-Supply Paper 1229.

GLOVER, R. E. and G. G. BALMER. 1954. River depletion resulting from pumping a well near a river. Trans. Am. Geophys. Union Vol. 35.

HANTUSH, M. S. 1959. Analysis of data from pumping wells near a river. Jour. Geophys. Res. Vol. 64.

HANTUSH, M. S. 1964. Hydraulics of Wells, in Advances in Hydro Science edited by V. T. Chow. Academic Press, New York.

HANTUSH, M. S. 1965. Wells near streams with semipervious beds. Jour. Geophys. Res. Vol. 70.

INGERSOLL, L. R., O. J. ZOBEL, and A. C. INGERSOLL. 1948. Heat conduction with engineering and geological applications. McGraw-Hill Book Co., New York.

JACOB, C. E. 1944. Notes on determining permeability by pumping tests under water table conditions. U. S. Geol. Survey mimeo. rept.

KARPLUS, W. J. 1958. Analog simulation. McGraw-Hill Book Co., Inc. New York.

KAZMIANN, R. G. 1948. The induced infiltration of river water to wells. Trans. Am. Geophys. Union. Vol. 29.

MILLMAN, JACOB and SAMUEL SEELY. 1941. Electronics. McGraw-Hill Book Co., Inc. New York.

ROBABAUGH, M. I. 1951. Stream-bed percolation in development of water supplies. Intern. Assoc. Sci. Hydrology, Genl. Assembly of Grussels, Vol. 2, Publ. 33.

ROBABAUGH, M. I. 1956. Ground-water resources of the northeastern part of the Louisville area, Ky: U. S. Geol. Survey Water-Supply Paper 1360-B.

SCHAEFER, E. J. and PAUL KASER. 1965. Graphical aids for the solution of formulas used in analyzing induced infiltration aquifer tests. Ohio Division of Water. Tech. Rept. No. 6.

SCHICHT, R. J. 1965. Ground-water development in East St. Louis area, Illinois. Illinois State Water Survey. Report of Investigation No. 51.

SKIBITZKE, H. E. 1961. Electronic computers as an aid to the analysis of hydrologic problems. Publ. 52. Internatl. Assn. of Scientific Hydrology.

STALLMAN, R. W. 1956. Numerical analysis of regional water levels to define aquifer hydrology. Trans. Am. Geophys. Union Vol. 37, No. 4.

THEIS, C. V. 1935. The relation between the lowering of the piezometric surface and the rate and duration of discharge of a well using ground-water storage: Am. Geophys. Union Trans., Pt. 2.

THEIS, C. V. 1941. The effect of a well on the flow of a nearby stream: Am. Geophys. Union Trans., Pt. 3.

WALTON, W. C. 1962. Selected analytical methods for well and aquifer evaluation. Illinois State Water Survey. Bulletin 49.

WALTON, W. C. 1963. Estimating the infiltration rate of a streambed by aquifer-test analysis. Internat. Assoc. Sci. Hydrology. Genl. Assembly of Berkeley.

WALTON, W. C. and T. A. PRICKETT. 1963. Hydrogeologic electric analog computers. Journ. Hyd. Div. ASCE.